TDA Progress Report 42-121

May 15, 1995

# Residual and Suppressed-Carrier Arraying Techniques for Deep-Space Communications

M. Shihabi, B. Shah, S. Hinedi, and S. Million
Communications Systems Research Section

*Three techniques that use carrier information from multiple antennas to enhance carrier acquisition and tracking are presented. These techniques in combination with baseband combining are analyzed and simulated for residual and suppressed-carrier modulation. It is shown that the carrier arraying using a single carrier loop technique can acquire and track the carrier even when any single antenna in the array cannot do so by itself. The carrier aiding and carrier arraying using multiple carrier loop techniques, on the other hand, are shown to lock on the carrier only when one of the array elements has sufficient margin to acquire the carrier on its own.*

## I. Introduction

Combining or arraying signals from multiple antennas has the advantage of increasing the signal-to-noise ratio (SNR) of the received signal. For example, it is well known [1] that ideally the SNR of the combined signal is the sum of the SNRs corresponding to the individual antennas. Practically, the achievable gain depends on the type of scheme being implemented as well as on the characteristics of the received signal. This article is mainly concerned with three similar techniques that first use information from multiple antennas to acquire and track the carrier, and then use baseband combining (BBC) [2] on the carrier demodulated signals to demodulate the subcarrier and detect the symbols. The three techniques, which work in conjunction with BBC, are carrier arraying using a single carrier loop, carrier arraying using multiple carrier loops, and carrier aiding. As will be shown shortly, the second and third techniques are usable for both residual and suppressed-carrier modulation. The carrier arraying with a single carrier loop followed by the baseband combining technique, however, is not practical for suppressed-carrier modulation. Practical implementations that demodulate an arrayed suppressed-carrier signal using a single carrier loop are the full-spectrum combining and/or complex symbol combining techniques described in [3].

The main difference between the techniques under consideration is that the first, carrier arraying using a single carrier loop, does not require any single antenna in the array to acquire and track the carrier by itself. The other two techniques, on the other hand, require at least one antenna in the array to lock the carrier on its own. The use of these techniques is best illustrated through an example. Consider an array of one 70-m and two standard (STD) 34-m antennas operating at S-band frequencies (2.2–2.3 GHz) [4]. A typical radio frequency spectrum of the received signal is shown in Fig. 1 in the absence of noise.

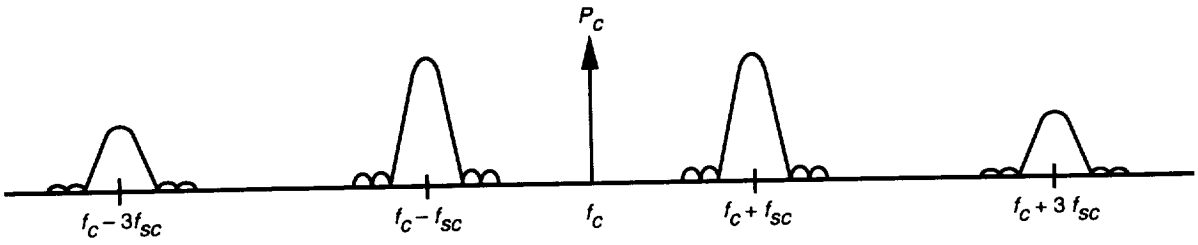


**Fig. 1. PCM/PSK/PM square-wave subcarrier signal model.**

Assume that $P_T/N_0$, the ratio of the total received power to the one-sided noise power spectral density (PSD) level, at the 70-m is 15 dB-Hz; the modulation index is 58 deg, and the symbol rate is 20 symbols per second (sps). Then, since the ratio of $P_T/N_0$ at the STD 34-m to that at the 70-m is $\gamma = 0.17$ [1], the $(P_T/N_0)_{34-m} = 7.3$ dB-Hz. (The ratios of $P_T/N_0$ of typical 34-m antennas in the DSN to the $P_T/N_0$ of the 70-m are shown in Table 1.) The corresponding $P_C/N_0$ are 9.5 dB-Hz for the 70-m and 1.8 dB-Hz for the 34-m. For this scenario, suppose that the minimum bandwidth required to track the carrier is 1 Hz, and the minimum loop SNR needed to reliably track the residual carrier is 7 dB [5]. Then the 70-m antenna with a carrier loop SNR of 9.5 dB can acquire the carrier, but the two 34-m antennas with loop SNRs of 1.8 dB are unable to do so. Applying the techniques described in this article, however, still enables us to make use of the information at the smaller antennas.

**Table 1. Gamma factors for DSN antennas.**

| Antenna size | Frequency band | $\gamma_i$ |
|---|---|---|
| 70-m | S-band | 1.00 |
| 34-m STD | S-band | 0.17 |
| 34-m HEF | S-band | 0.07 |
| 70-m | X-band | 1.00 |
| 34-m STD | X-band | 0.13 |
| 34-m HEF | X-band | 0.26 |

Let us discuss the techniques one at a time. Carrier aiding is shown in Fig. 2. Here the 70-m (or master) antenna in the array first locks the carrier and then passes its reference to the other (34-m) antennas. At the 34-m antenna, the received signal is first delayed to time align it with the 70-m signal, then open-loop downconverted to baseband using the 70-m reference, and subsequently coherently demodulated using a baseband phase-locked loop (PLL). (Note that we arbitrarily assume the signal at the 34-m antenna to be delayed relative to the 70-m antenna.) When the antennas in the array are colocated, the baseband PLLs can operate at bandwidths much narrower than otherwise possible, because most of the signal dynamics are removed by the master reference signal in the downconversion to baseband. In the case of the example given, the baseband PLL would be able to use a bandwidth much narrower than 1 Hz, because it must only track the residual Doppler between the 70-m antenna and 34-m antennas. The narrow bandwidth results in an increased loop SNR, which allows the 34-m antennas to lock the carrier. In this example, if the modulation index were changed to 90 deg so that the carrier is fully suppressed, the technique in Fig. 2 could still be used by using a Costas loop instead of a PLL to track the carrier.

Note that carrier aiding is only useful when at least one antenna is able to acquire the carrier on its own. If this requirement is not met, a different technique, such as carrier arraying using a single carrier loop, is needed. We begin with the implementation shown in Fig. 3. Here the time-aligned residual carrier

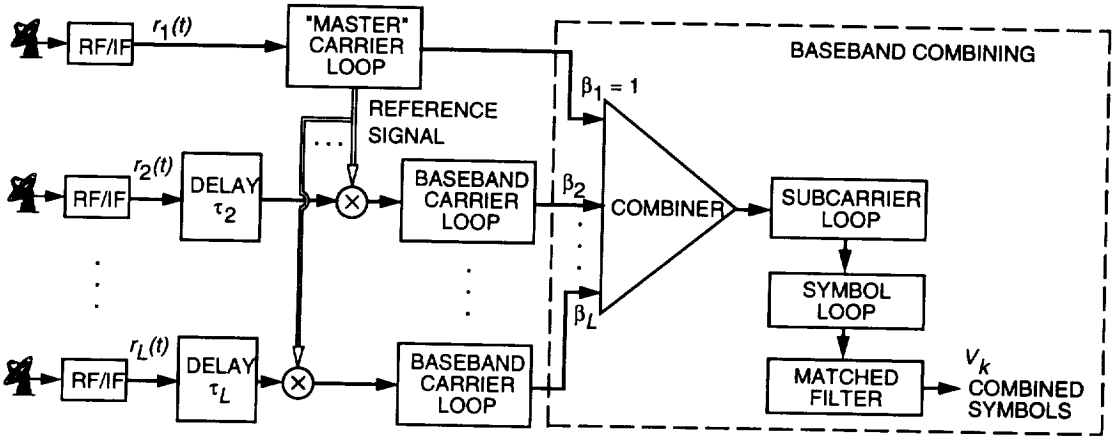


**Fig. 2. Carrier aiding/BBC: system overview.**

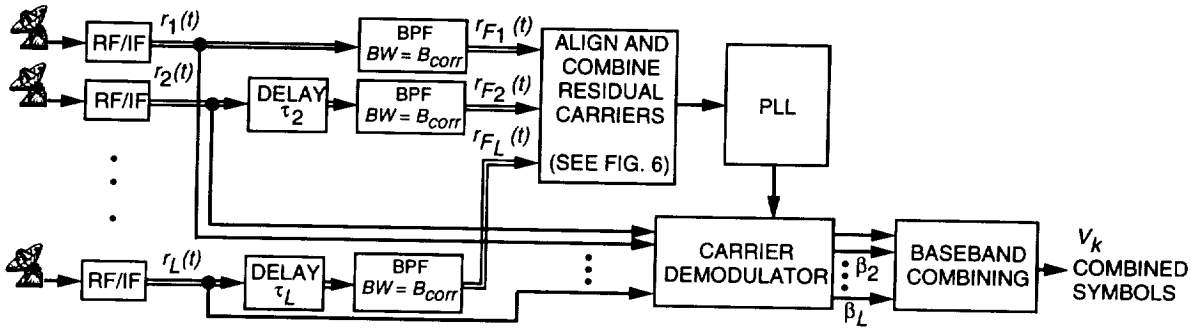


**Fig. 3. CA/single PLL: system overview.**

component at each antenna is filtered and transmitted to a central location, phase aligned, combined, and input to a single carrier loop. As a result, for a given bandwidth, the loop will lock the carrier provided the combined signal has sufficient $P_C/N_0$. Ideally, the combined $P_C/N_0$ is the sum of $P_C/N_0$ at the individual antennas. Consider the same scenario as before but with the 70-m antenna replaced by two additional 34-m STD antennas. Under this scenario, carrier aiding cannot be implemented using a 1-Hz loop, as none of the four 34-m antennas has sufficient $P_C/N_0$ to lock the carrier. However, carrier arraying using a single PLL with a 1-Hz bandwidth can be implemented since the combined $P_C/N_0$ of the four 34-m antennas is 7.8 dB-Hz. When there is no residual component at $f = f_c$ in Fig. 1, the implementation shown in Fig. 3 cannot be used without modification. The simplest way to handle this case would be to widen the bandwidth of the bandpass filter (BPF) in Fig. 3 so that it passes the first $N$ harmonics of the telemetry signal. The harmonics from each antenna would then be transmitted to a central location, aligned, combined, and tracked by replacing the PLL in Fig. 3 with a Costas loop. Note that the modified implementation is impractical because it requires the signal to be combined twice: first, as just described, for carrier tracking and then for baseband demodulation. A more practical implementation along these lines is full-spectrum combining (FSC) [3], where the signal is combined at IF and then tracked using a single receiver. An altogether different approach that also uses a single carrier loop but multiple subcarrier and symbol loops is complex symbol combining (CSC) [3].

Finally, we turn to the carrier-arraying with multiple PLLs technique shown in Fig. 4. As will shortly be shown, this technique can be viewed as a hybrid of the techniques in Figs. 2 and 3. Here, as in Fig. 2, the received signal at each antenna (except the master) is first downconverted to baseband using the master antenna carrier reference and coherently tracked using a baseband PLL. As before, due to rate aiding by the master, the baseband PLL operates at narrower bandwidths and a higher loop SNR than

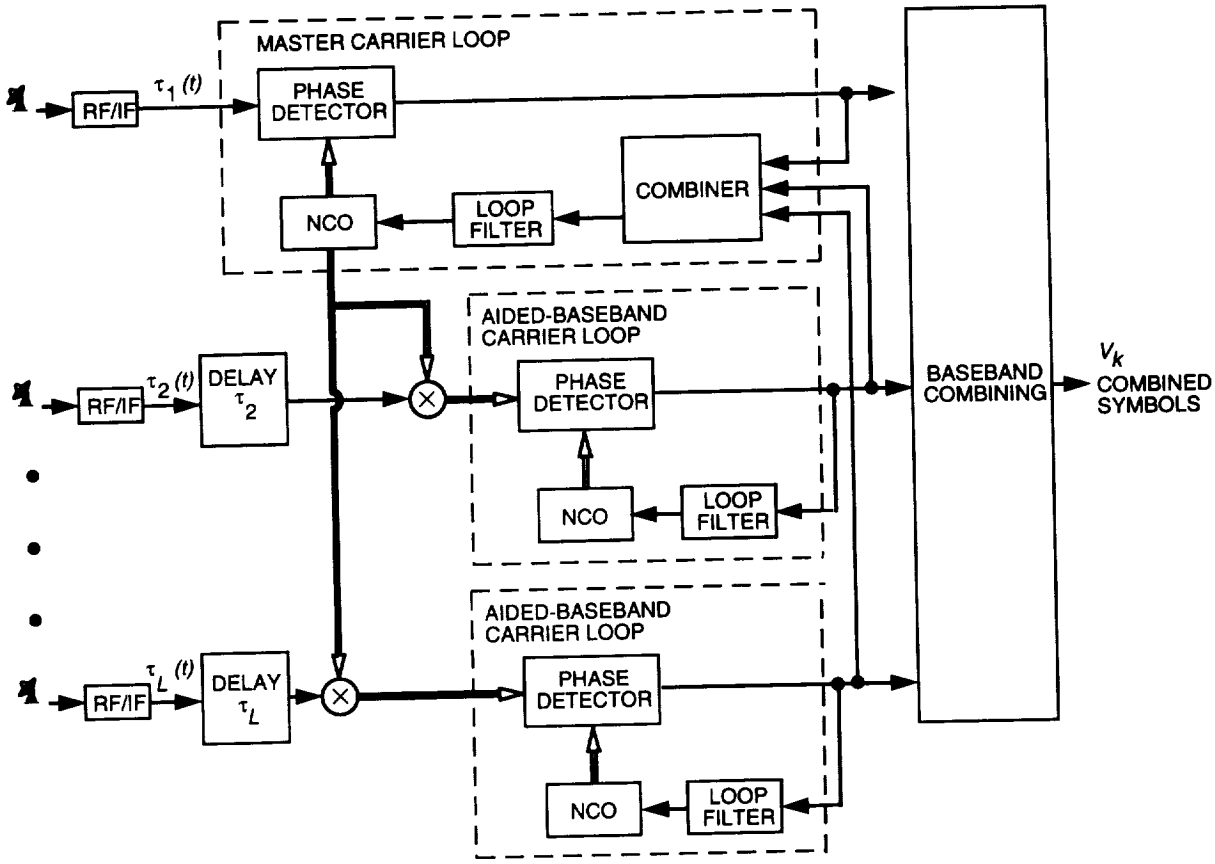


**Fig. 4. CA/multiple PLLs: system overview.**

in the absence of rate aiding. However, now the master antenna also benefits, because the error signal from each of the other antennas is added to its error signal. Hence, when all the loops are tracking, the master PLL also operates at a loop SNR that is improved. In the upper limit, when all the error signals add coherently, the loop SNR of the master is equal to the ideal loop SNR of the carrier-arraying with the single PLL technique in Fig. 3. In practice, we can expect the performance of this scheme to be better than carrier aiding but not as good as carrier-arraying with a single PLL. Note that if the master cannot acquire the signal on its own, it cannot rate aid the other antennas, and this scheme is unusable. In the examples considered earlier, this technique would work well for an array of one 70-m and two STD 34-m antennas, but would not be implementable for an array of four STD 34-m antennas that cannot lock individually. This scheme can be used for suppressed-carrier modulation by replacing the PLL with the Costas loop.

In this article, the tracking performance of all three techniques is measured in terms of SNR degradation and symbol SNR loss. Both performance measures have been explained in detail earlier [3]. Briefly, SNR degradation is defined as the ratio of the SNR at the matched filter output in the presence of nonideal synchronization to the SNR in the presence of ideal synchronization. Symbol SNR loss is defined as the additional symbol SNR needed by a system with synchronization errors to achieve the same symbol error rate (SER) as one with no synchronization errors. In the following sections, analytical expressions are derived to describe the performances of carrier arraying using a single PLL and carrier aiding. The performances of these systems were also obtained via simulations and seen to agree closely with the theory. Performance for carrier arraying using multiple PLLs is obtained via simulation only.

## II. Single Receiver Performance

We begin with the performance of a single receiver, as it is the basis for the analysis of the schemes in Figs. 1 through 3. In deep-space communications, the downlink symbols are first modulated onto a square-wave subcarrier that, in turn, modulates an RF carrier [6]. As shown in Fig. 1, this has the advantage of transmitting a residual carrier component whose frequency does not coincide with the data spectrum. In general, the downlink deep-space signal can be represented as [6]

$$r(t) = \sqrt{2P_T}\sin\left[\omega_c t + \delta\, d(t)\ \mathrm{Sqr}(\omega_{sc}t + \theta_{sc}) + \theta_c\right] + n(t) \tag{1}$$

where $P_T$ is the total received power in watts (W), and $\omega_c$ and $\theta_c$ are the carrier angular frequency in radians per second (rad/s) and phase in rad, respectively. The $\mathrm{Sqr}(\omega_{sc}t + \theta_{sc}) = \mathrm{sgn}(\sin(\omega_{sc}t + \theta_{sc}))$ is the square-wave subcarrier with angular frequency $\omega_{sc}$ rad/s and phase $\theta_{sc}$ rad. The signum function sgn $(x)$ equals $+1$ when its argument is positive and $-1$ otherwise. The modulation index, $\delta$, ranges from 0 to $\pi/2$. The carrier power $P_C = P_T\cos^2\delta$, and the data power $P_D = P_T\sin^2\delta$. When $\delta = \pi/2$, the signal is "suppressed-carrier" modulated. In this case, the downlink signal spectrum is as given in Fig. 1, but without the residual carrier at $f_c$. The symbol stream, $d(t)$, is given by

$$d(t) = \sum_{k=-\infty}^{\infty} d_k p(t - kT) \tag{2}$$

where $d_k$ is the $\pm 1$ binary data for the $k$th symbol and $T$ is the symbol period in seconds. The baseband pulse, $p(t)$, is unity in $[0,T)$ and zero otherwise. The bandpass noise, $n(t)$, can be written as

$$n(t) = \sqrt{2}n_c(t)\cos(\omega_c t) - \sqrt{2}n_s(t)\sin(\omega_c t) \tag{3}$$

where $n_c(t)$ and $n_s(t)$ are statistically independent, stationary, band-limited, white Gaussian low-pass noise processes with one-sided PSD level $N_0$ (W/Hz) and one-sided bandwidth $W_n$ (Hz).

As shown in Fig. 5, the deep-space signal is demodulated using a receiving chain consisting of a carrier-tracking loop, a subcarrier-tracking loop, and a symbol-synchronizer loop. If $\delta < \pi/2$, a PLL is used for carrier tracking. When $\delta = \pi/2$, however, carrier tracking is achieved using a Costas loop. Computation of the degradation and loss begins with the expression for the soft symbols, $v_k$, in Fig. 5. From [1,6],

$$v_k = \begin{cases} \sqrt{P_D}C_c C_{sc} d_k + n_k & d_k = d_{k-1} \\ \sqrt{P_D}C_c C_{sc}\left(1 - \dfrac{|\phi_{sy}|}{\pi}\right) d_k + n_k & d_k \neq d_{k-1} \end{cases} \tag{4}$$

where the noise $n_k$ is Gaussian with variance $\sigma_n^2 = N_0/(2T)$. The signal reduction functions $C_c$ and $C_{sc}$ are due to imperfect carrier and subcarrier synchronization and are given as [1,6]

$$C_c = \cos\phi_c \tag{5}$$

$$C_{sc} = 1 - \frac{2}{\pi}|\phi_{sc}| \tag{6}$$

where $\phi_c$ and $\phi_{sc}$ denote the carrier and subcarrier phase tracking errors, respectively. The symbol timing error, $\phi_{sy}$, which affects the output only when there is a symbol transition (i.e., when $d_k \neq d_{k+1}$), reduces


**Fig. 5. Single receiver: overview.**

the signal amplitude by $1 - (|\phi_{sy}|/\pi)$. Ideally, $\phi_c = \phi_{sc} = \phi_{sy} = 0$ and Eq. (4) reduces to the familiar matched filter output $v_{k,ideal} = \sqrt{P_D}d_k + n_k$, as expected. In writing Eq. (4), it is assumed that the carrier, subcarrier, and symbol loop bandwidths are much smaller than the symbol rate so that the phase errors $\phi_c$, $\phi_{sc}$, and $\phi_{sy}$ can be modeled as constant over several symbols.

Throughout this article, the density function of $\phi_c$ is assumed to be Tikhonov,[1] that is,

$$p_c(\phi_c) = \begin{cases} \dfrac{\exp(\rho_c \cos\phi_c)}{2\pi I_o(\rho_c)} & |\phi_c| \le \pi \quad \text{residual-carrier case} \\ \dfrac{\exp((1/4)\rho_c \cos 2\phi_c)}{\pi I_o((1/4)\rho_c)} & |\phi_c| \le \dfrac{\pi}{2} \quad \text{suppressed-carrier case} \\ 0 & \text{otherwise} \end{cases} \tag{7}$$

where $I_k(x) = 1/\pi \int_0^\pi e^{x\cos\theta}\cos(k\theta)d\theta$ is the modified Bessel function of order $k$, and $\rho_c$ is the carrier loop SNR. From [7],

$$\rho_c = \begin{cases} \dfrac{P_C/N_0}{B_c} & \text{residual-carrier case} \\ \dfrac{P_D/N_0}{B_c}\left(1 + \dfrac{1}{2E_s/N_0}\right)^{-1} & \text{suppressed-carrier case} \end{cases} \tag{8}$$

where the symbol SNR $E_s/N_0 = P_D T/N_0$ and $B_c$ Hz is the carrier loop bandwidth. The subcarrier and symbol densities, $p_{sc}(\phi_{sc})$ and $p_{sy}(\phi_{sy})$, are assumed to be Gaussian. Hence,

$$p_i(\phi_i) = \frac{\exp(-\phi_i^2/2\sigma_i^2)}{\sqrt{2\pi\sigma_i}}, \qquad i = sc, sy \tag{9}$$

where $\sigma_{sc}^2$ is the reciprocal of the subcarrier loop SNR, $\rho_{sc}$, and $\sigma_{sy}^2$ is the reciprocal of the symbol loop SNR, $\rho_{sy}$. The subcarrier [7] and symbol [8] loop SNRs are respectively given as

$$\rho_{sc} = \left(\frac{2}{\pi}\right)^2 \frac{P_D/N_0}{W_{sc}B_{sc}}\left(1 + \frac{1}{2E_s/N_0}\right)^{-1} \tag{10}$$

$$\rho_{sy} = \frac{P_D/N_0}{2\pi^2 W_{sy}B_{sy}} \times \frac{\left(\operatorname{erf}\left(\sqrt{E_s/N_0}\right) - (W_{sy}/(2\sqrt{\pi}))\sqrt{E_s/N_0}\exp\left(-(E_s/N_0)\right)\right)^2}{\left(1 + (E_s/N_0)(W_{sy}/2) - (W_{sy}/2)\left[(1/\sqrt{\pi})\exp\left(-(E_s/N_0)\right) + \sqrt{E_s/N_0}\operatorname{erf}\left(\sqrt{E_s/N_0}\right)\right]^2\right)} \tag{11}$$

[1] It is assumed that the Costas loop locks at zero phase error. The $\pi$ lock point can be handled by an appropriate transformation [6].

where $\text{erf}(x) = (2/\sqrt{\pi}) \int_0^x \exp(-v^2)dv$ is the error function, and $B_{sc}$ and $B_{sy}$ (in Hz) denote the single-sided subcarrier and symbol loop bandwidths, respectively. The parameters $W_{sc}$ and $W_{sy}$, which denote the subcarrier and symbol window, are unitless and limited to $(0, 1]$.

A useful quantity needed to compute degradation and loss is the symbol SNR conditioned on $\phi_c$, $\phi_{sc}$, and $\phi_{sy}$. The conditional symbol SNR, denoted by $SSNR'$, is defined as the square of the conditional mean of $v_k$ divided by the conditional variance of $v_k$, i.e.,

$$SSNR' = \frac{\overline{(v_k/\phi_c, \phi_{sc}, \phi_{sy})}^2}{\sigma_n^2}$$

$$= \begin{cases} \dfrac{2P_D T}{N_0} C_c^2 C_{sc}^2 & d_k = d_{k-1} \\ \dfrac{2P_D T}{N_0} C_c^2 C_{sc}^2 \left(1 - \dfrac{|\phi_{sy}|}{\pi}\right)^2 & d_k \neq d_{k-1} \end{cases} \tag{12}$$

where $\overline{(x/y)}$ denotes the statistical expectation of $x$ conditioned on $y$, and $v_k$ and $\sigma_n^2$ are defined earlier.

### A. Degradation

The symbol SNR degradation is defined as the symbol SNR at the matched filter output in the presence of imperfect synchronization divided by the ideal matched filter output SNR. The nonideal symbol SNR, denoted as $SSNR$, is found by first averaging Eq. (12) over the symbol transition probability and then over the carrier, subcarrier, and symbol phases. It can be shown that [1]

$$SSNR = \frac{2P_D T}{N_0} \overline{C_c^2}\ \overline{C_{sc}^2}\ \overline{C_{sy}^2} \tag{13}$$

where the signal amplitude reduction due to symbol timing errors is denoted $C_{sy}$ and given as

$$C_{sy} = 1 - \frac{|\phi_{sy}|}{2\pi} \tag{14}$$

for a transition probability of one-half. The average of the signal reduction functions is [1]

$$\overline{C_c^2} = \begin{cases} \dfrac{1}{2}\left[1 + \dfrac{I_2(\rho_c)}{I_0(\rho_c)}\right] & \text{residual-carrier case} \\ \dfrac{1}{2}\left[1 + \dfrac{I_1((1/4)\rho_c)}{I_0((1/4)\rho_c)}\right] & \text{suppressed-carrier case} \end{cases} \tag{15}$$

$$\overline{C_{sc}^2} = 1 - \sqrt{\frac{32}{\pi^3}} \frac{1}{\sqrt{\rho_{sc}}} + \frac{4}{\pi^2} \frac{1}{\rho_{sc}} \tag{16}$$

$$\overline{C_{sy}^2} = 1 - \sqrt{\frac{2}{\pi^3}} \frac{1}{\sqrt{\rho_{sy}}} + \frac{1}{4\pi^2} \frac{1}{\rho_{sy}} \tag{17}$$

Ideally, when there are no phase errors (i.e., when $\rho_c = \rho_{sc} = \rho_{sy} = \infty$), $\overline{C_c^2} = \overline{C_{sc}^2} = \overline{C_{sy}^2} = 1$ and Eq. (13) reduces to $SSNR_{ideal} = 2P_DT/N_0$, as expected. The degradation, $D$, for a single antenna is thus given by

$$D = 10\log_{10}\left(\frac{SSNR}{SSNR_{ideal}}\right) = \log_{10}\overline{C_c^2}\;\overline{C_{sc}^2}\;\overline{C_{sy}^2} \tag{18}$$

Note that the degradation defined in this way is a negative number.

### B. Loss

The SER for the single receiver in Fig. 5, denoted $P_s(E)$, is defined as [2,3]

$$P_s(E) = \int_{\phi_c}\int_{\phi_{sc}}\int_{\phi_{sy}} P_s'(E)p_c(\phi_c)p_{sc}(\phi_{sc})p_{sy}(\phi_{sy})d\phi_{sy}d\phi_{sc}d\phi_c = f\left(\sqrt{\frac{E_s}{N_0}}\right) \tag{19}$$

where $f(\cdot)$ is the functional relationship between SER and $\sqrt{E_s/N_0}$. The quantity $P_s'(E)$ is the SER conditioned on the phase errors $\phi_c$, $\phi_{sc}$, and $\phi_{sy}$. Following similar steps as in [9], the conditional SER can be shown to be

$$P_s'(E) = \frac{1}{4}\,\text{erfc}\,\left(\sqrt{SSNR' \text{ when } d_k \neq d_{k-1}}\right) + \frac{1}{4}\,\text{erfc}\,\left(\sqrt{SSNR' \text{ when } d_k = d_{k-1}}\right) \tag{20}$$

where

$$\text{erfc}\,(x) = \frac{2}{\sqrt{\pi}}\int_x^\infty \exp(-v^2)dv = 1 - \text{erf}(x) \tag{21}$$

is the complementary error function. Substituting Eq. (12) for $SSNR'$ in Eq. (20) yields

$$P_s'(E) = \frac{1}{4}\,\text{erfc}\,\left[\sqrt{\frac{E_s}{N_0}}C_cC_{sc}\left(1 - \frac{|\phi_{sy}|}{\pi}\right)\right] + \frac{1}{4}\,\text{erfc}\,\left[\sqrt{\frac{E_s}{N_0}}C_cC_{sc}\right] \tag{22}$$

Ideally, when there are no timing errors, Eq. (19) reduces to the well-known binary phase shift keyed (BPSK) error rate, $P_s(E) = 1/2\,\text{erfc}\,(\sqrt{E_s/N_0})$.

Symbol SNR loss is defined as the additional symbol SNR needed in the presence of imperfect synchronization to achieve the same SER as in the presence of perfect synchronization. Mathematically, the SNR loss due to imperfect carrier, subcarrier, and symbol timing references is given in dB as

$$L = 20\log\left[f^{-1}(P_s(E))\right]|_{[\text{infinite loop SNR}]} - 20\log\left[f^{-1}(P_s(E))\right]|_{[\text{finite loop SNR}]} \tag{23}$$

where $f(\cdot)$ and $P_s(E)$ are as defined by Eq. (19). The first term in Eq. (23) is the value of $E_s/N_0$ required at a given value of $P_s(E)$ in the presence of perfect synchronization, whereas the second term is the value of $E_s/N_0$ required for imperfect synchronization. Note that loss defined in this way is a negative number.

## III. Carrier Array Using a Single PLL

Carrier arraying using a single PLL followed by BBC is shown in Fig. 3. This scheme is similar to the single receiver in that signal demodulation uses a single PLL, subcarrier loop, and symbol loop. Two main differences, however, are (1) the IF residual carrier signals are combined so that the PLL operates at a higher loop SNR than in the single receiver case, and (2) after carrier demodulation, the baseband signals are also combined so the subcarrier and symbols operate at a higher loop SNR as well.

Due to different path lengths, the received signal at antenna $i$ is delayed by $\tau_i$ s relative to antenna 1. After complex downconversion to an appropriate IF, the signal at antenna $i$ can be represented as [1]

$$\begin{aligned} r_i(t) &= r_1(t-\tau_i) \\ &= \sqrt{P_{T_i}} \exp\{j[\omega_I t - \omega_c \tau_{i1} + \delta d(t-\tau_i)\ \mathrm{Sqr}[\omega_{sc}(t-\tau_i)+\theta_{sc_i}] + \theta_{c_i}]\} \\ &\quad + n_i(t)\exp\{j[\omega_I t + \theta_{c_i}]\} \end{aligned} \tag{24}$$

where for an $L$-antenna array, $i = 1, 2, \cdots, L$. The carrier phase of the $i$th signal is $\theta_{c_i}(t) = \theta_{c_1}(t) + \Delta\theta_i(t)$ where $\Delta\theta_i$ represents the differential Doppler between the signal $i$ and the signal 1. (Antenna 1 has arbitrarily been chosen as the reference antenna.) All other parameters in Eq. (24) are as defined in Eq. (1), except for $\omega_I$, which denotes the carrier IF frequency. Here the noise $n_i(t)$ is a complex noise process with a one-sided PSD level equal to $2N_0$ (W/Hz). As shown in Fig. 3, each IF signal is first filtered to extract the carrier component and then transmitted to a central location where it is phase aligned and combined with carrier signals from other antennas. The phase alignment and combining algorithms are shown in Figs. 6 and 7. Note that the combining algorithm here is almost identical to that used for the full-spectrum combining technique described in [1,3], the difference being that here the output of the bandpass filter in Fig. 3 is the residual carrier component, whereas in [1,3] it was the first $N$ harmonics of the telemetry signal. The filter output, $r_{F_i}(t)$ in Fig. 6, is given as

$$r_{F_i}(t) = \sqrt{P_{C_i}} \exp[j(\omega_I t + \theta_{c_i})] + n_{F_i}(t)\exp[j(\omega_I t + \theta_{c_i})] \tag{25}$$

for $i = 1, \cdots, L$. Here $P_{C_i}$ is the received carrier power at antenna $i$, and the noise $n_{F_i}(t)$ is a complex bandpass Gaussian noise. The signals $r_{F_i}(t)$ $(i \neq 1)$ are phase aligned with $r_{F_1}(t)$, scaled by the optimum weighting factors [2,10], $\beta_i = (\sqrt{P_{C_i}} N_{01})/(\sqrt{P_{C_1}} N_{0i})$, and then combined. Combining the carrier signals in this way maximizes the combining gain [10].

Let $\theta_{i1} = \Delta\theta_i$ denote the phase difference between signal $i$ and the reference signal before phase alignment. Then the signal $r_{F_i}(t)$ is aligned with the reference $r_{F_1}(t)$ by rotating $r_{F_i}(t)$ by $e^{-j\hat{\theta}_{i1}}$ for $i = 2, \cdots, L$. The estimate [11], $\hat{\theta}_{i1}$, is obtained using the algorithm in Fig. 7. Denote the phase alignment error $\Delta\phi_{i1} = \theta_{i1} - \hat{\theta}_{i1}$. Then the variance of $\Delta\phi_{i1}$ is related to the SNR of the phase difference estimator by [1,3,11]

$$\sigma^2_{\Delta\phi_{i1}} \approx \frac{1}{2\ SNR_{i1}} \tag{26}$$

where [11]

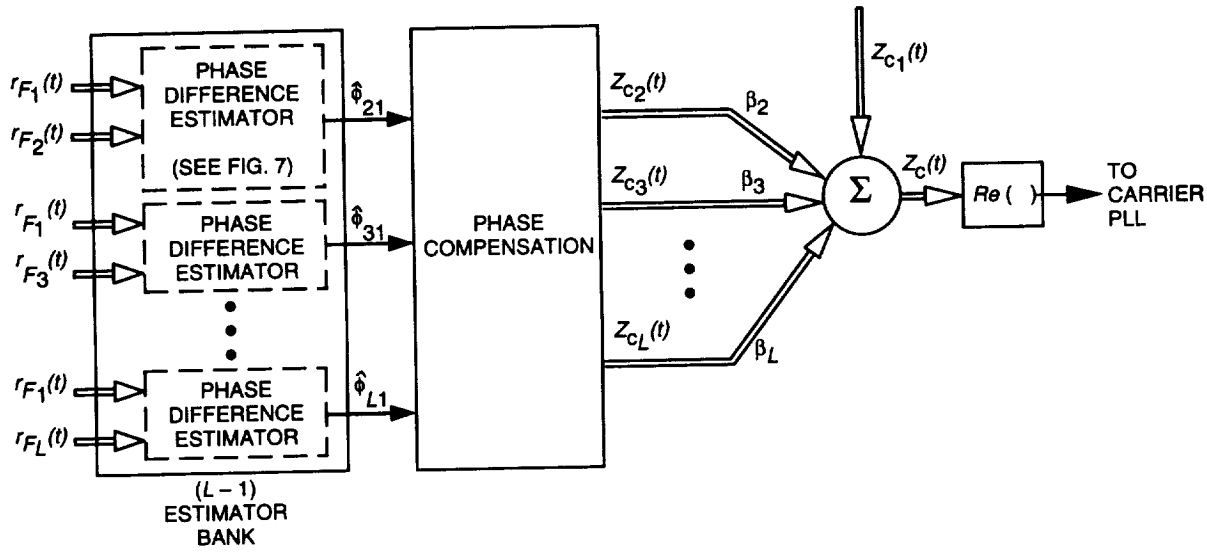


Fig. 6. The carrier maximal-ratio combining bank.

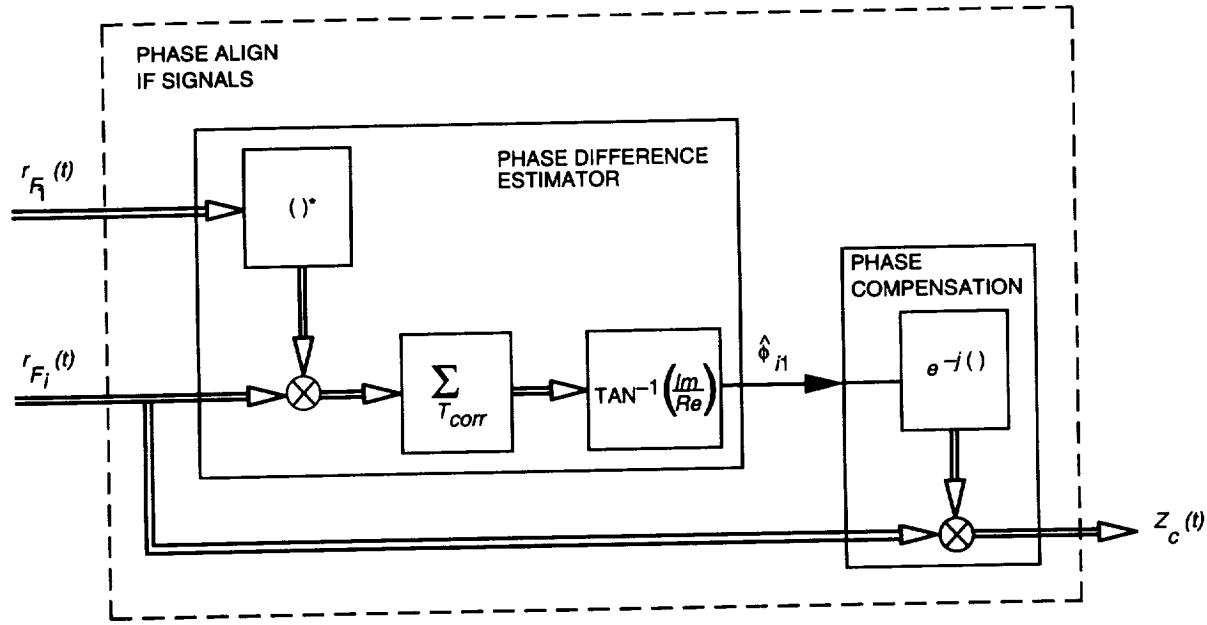


Fig. 7. Phase alignment and combining of two carrier signals.

$$SNR_{i1} = \frac{2T_{corr}((P_{C_1})/(N_{01}))}{1 + (1/\gamma_i) + B_{corr}[1/((P_{C_i})/(N_{oi}))]} \tag{27}$$

The parameter $B_{corr}$ denotes the single-sided bandwidth of the BPF in Fig. 3, $T_{corr}$ denotes the estimation interval, and the ratio $\gamma_i = (P_{C_i}/P_{C_1})(N_{01}/N_{0i})$ is called the antenna gamma factor. These ratios are shown in Table 1 for several DSN antennas operating in S-band or X-band (8.4–8.5 GHz).

The IF carrier signals after phase compensation, denoted $Z_{C_i}(t)$ in Fig. 6, are given as

$$Z_{C_i}(t) = \sqrt{P_{C_i}} e^{j[\omega_I t + \theta_1(t) + \Delta\phi_{i1}(t)]} + n_i(t) e^{j[\omega_I t + \theta_1(t) + \Delta\phi_{i1}(t)]} \tag{28}$$

The combined signal, $Z_C(t)$, obtained by taking the weighted sum of $Z_{C_i}(t)$ is a complex tone plus noise. Namely,

$$Z_C(t) = \sum_{i=1}^{L} \beta_i Z_{C_i}(t) \tag{29}$$

Following the same steps as in [1,3], the power of the complex tone in Eq. (29) averaged over $\Delta\phi_{i1}$ can be shown to be

$$P_{C_{comb}} = P_{C_1} \sum_{i=1}^{L} \sum_{j=1}^{L} \gamma_i \gamma_j \overline{C_{ij}} \tag{30}$$

where $\overline{C_{ij}}$, the average signal reduction function due to phase misalignment between the signal $i$ and the signal $j$, is given as [1,3]

$$\overline{C_{ij}} = \begin{cases} e^{-(1/2)[\sigma^2_{\Delta\phi_{i1}} + \sigma^2_{\Delta\phi_{j1}}]} & m \neq n \\ 1 & m = n \end{cases} \tag{31}$$

Similarly, the one-sided PSD level of the combined noise at the carrier loop input is given by [2]

$$2N_{0_{eff}} = 2\ N_{01} \sum_{i=1}^{L} \gamma_i \tag{32}$$

Referring to Fig. 6, the PLL input is formed by taking the real part of the combined signal $Z_C(t)$. Consequently, the PLL loop SNR is given by

$$\begin{aligned} \rho_c &= \frac{P_{C_{comb}}/N_{0_{eff}}}{B_c} \\ &= \frac{P_{C_1}/N_{0_1}}{B_c} \left[ \frac{\sum_{i=1}^{L} \gamma_i^2 + \sum_{i=1}^{L} \sum_{\substack{j=1 \\ i \neq j}}^{L} \gamma_i \gamma_j \overline{C_{ij}}}{\sum_{i=1}^{L} \gamma_i} \right] \end{aligned} \tag{33}$$

where the bracketed term is the improvement in loop SNR due to arraying.

### A. Carrier Demodulation

Since the PLL input is formed by aligning the phase of signals 2 through $L$ with the phase of signal 1, the PLL reference is tuned to signal 1 and can be used without modification to demodulate the carrier at antenna 1. Carrier demodulation at antenna $i$ (for $i \neq 1$), however, can be performed only after aligning the phase of the PLL reference to that of the carrier at antenna $i$. That is, carrier demodulation at antenna $i$ is performed after rotating the PLL reference by $e^{j\hat{\theta}_{i1}}$. Also note that since the carrier reference at all antennas is derived from a single carrier loop, the SNR degradation and loss due to

imperfect carrier synchronization is the same for all antennas. That is, in the telemetry channel, the carrier signal reduction function for antenna $i$, denoted by $C_{c_i}$, is given by

$$C_{c_i} = \cos\phi_c \qquad i = 1, 2, \cdots, L \tag{34}$$

where $\sigma^2_{\phi_c} = 1/\rho_c$, and $\rho_c$ is given by Eq. (33).

Assume that the baseband combiner in Fig. 3 perfectly time aligns the signals before combining them;[2] then, following the same steps as in [1,11], it can be shown that the combined symbol stream at the matched filter output can be written as

$$v_k = \begin{cases} \sqrt{P_{D_1}\, g_{comb}} C_c C_{sc} d_k + n_k & d_k = d_{k-1} \\ \sqrt{P_{D_1}\, g_{comb}} C_c C_{sc} \left(1 - \dfrac{|\phi_{sy}|}{\pi}\right) d_k + n_k & d_k \neq d_{k-1} \end{cases} \tag{35}$$

where the conditional gain factor, denoted $g_{comb}$, is given by

$$g_{comb} = \sum_{n=1}^{L} \gamma_n^2 + \sum_{n=1}^{L} \sum_{\substack{m=1 \\ n \neq m}}^{L} \gamma_n \gamma_m C_{nm} \tag{36}$$

and the noise $n_k$ is a Gaussian random variable with variance $\sigma_n^2 = N_{0_e ff}/2T$. Defining the conditional symbol SNR as before yields

$$SSNR' = \begin{cases} \dfrac{2P_{D_1}T}{N_{01}} C_{comb} C_c^2 C_{sc}^2 & d_k = d_{k-1} \\ \dfrac{2P_{D_1}T}{N_{01}} C_{comb} C_c^2 C_{sc}^2 \left(1 - \dfrac{|\phi_{sy}|}{\pi}\right)^2 & d_k \neq d_{k-1} \end{cases} \tag{37}$$

where

$$C_{comb} = \frac{\sum_{n=1}^{L} \gamma_n^2 + \sum_{n=1}^{L} \sum_{\substack{m=1 \\ n \neq m}}^{L} \gamma_n \gamma_m C_{nm}}{\sum_{n=1}^{L} \gamma_n} \tag{38}$$

is the degradation due to imperfect phase alignment. The last equation is useful in computing the symbol SNR degradation and SER loss as shown below.

### B. Degradation

The SSNR degradation is defined as the ratio of the SSNR in the presence of imperfect phase alignment and synchronization to the ideal SSNR (no phase errors). The degradation is obtained by computing the SSNR in the presence of phase errors (averaging Eq. (37) over $\Delta\phi_{i1}$, $\phi_c$, $\phi_{sc}$, and $\phi_{sy}$) and then dividing that result by the ideal SSNR ($SSNR_{ideal} = ((2P_{D_1}T)/(N_{01}))\sum_{i=1}^{L}\gamma_i$). Hence,

[2] This assumption simplifies the analysis without affecting the relative performance of the schemes. Note that the uncombined signals are not assumed to be perfectly phase aligned.

$$D = 10\log_{10}\left[\overline{C_c^2}\;\overline{C_{sc}^2}\;\overline{C_{sy}^2}\left(\frac{\sum_{m=1}^{L}\gamma_m^2 + \sum_{m=1}^{L}\sum_{\substack{n=1\\n\neq m}}^{L}\gamma_m\gamma_n\overline{C_{mn}}}{(\sum_{m=1}^{L}\gamma_m)^2}\right)\right] \tag{39}$$

where $\overline{C_{nm}}$ is given by Eq. (31). The quantities $\overline{C_c^2}$, $\overline{C_{sc}^2}$, and $\overline{C_{sy}^2}$ are given by Eqs. (15) through (17) with the modification that the loop SNRs $\rho_c$, $\rho_{sc}$, and $\rho_{sy}$ presented in Eqs. (8) through (11) are now computed using the combined power-to-noise level, or $P_C/N_{0_{eff}}$, which is found from Eqs. (30) and (32).

### C. Loss

The SER for the array in Fig. 3 is computed using the same procedure as in the single receiver case. Therefore, the SER is given by averaging the conditional SER over all the phase errors. Assuming that the phase alignment errors, $\Delta\phi_{i1}$, are independent for $i = 1, \cdots, L$ we have [3]

$$P_s(E) = \int_{\phi_c}\int_{-\infty}^{\infty}\int_{-\infty}^{\infty}\underbrace{\int_{-\infty}^{\infty}\cdots\int_{-\infty}^{\infty}}_{L-1} P_s'(E)\times\left[p(\phi_c)p(\phi_{sc})p(\phi_{sy})\times\left(\prod_{n=2}^{L}p(\Delta\phi_{n1})\right)\right]\mathbf{d\Delta\phi}\,d\phi_{sy}\,d\phi_{sc}\,d\phi_c \tag{40}$$

where $\mathbf{\Delta\phi} = (\Delta\phi_{21}, \cdots, \Delta\phi_{L1})$ are the resulting $L-1$ phase alignment errors. The $\mathbf{\Delta\phi}$ are independent and identically distributed Gaussian random variables with variance given by Eq. (26). The statistics of the error processes $\phi_c$, $\phi_{sc}$, and $\phi_{sy}$ were described earlier. After substituting Eq. (37) in Eq. (20), the conditional SER becomes

$$P_s'(E) = \frac{1}{4}\,\mathrm{erfc}\left[\sqrt{\frac{E_{s1}}{N_{01}}C_{comb}}C_cC_{sc}\left(1-\frac{|\phi_{sy}|}{\pi}\right)\right] + \frac{1}{4}\,\mathrm{erfc}\left[\sqrt{\frac{E_{s1}}{N_{01}}C_{comb}}C_cC_{sc}\right] \tag{41}$$

where $E_{s1}/N_{01} = P_{D_1}T/N_{01}$ is the symbol SNR at antenna 1. Ideally, when there is no combining and the synchronization errors $C_{comb} = C_c = C_{sc} = 1 - |\phi_{sy}|/\pi = 1$, the SER given in Eq. (40) reduces to the well known BPSK symbol error rate, $P_s(E) = 1/2\ \mathrm{erfc}\ (\sqrt{E_{s1}/N_{01}(\sum_{n=1}^{L}\gamma_n)})$, where $(\sum_{n=1}^{L}\gamma_n)$ is the ideal combining gain. The SNR loss is given by Eq. (23) after using Eq. (40) for $P_s(E)$.

### D. Numerical Examples

The use of Eqs. (39) and (40) is illustrated here by computing the degradation and loss for the system in Fig. 3 when $L = 2$ and 4.

**1. Array of One 70-m and One STD 34-m Antenna.** Consider again an array of one 70-m and one STD 34-m antenna operating at S-band. Then from Table 1, with $\gamma_1 = 1$ and $\gamma_2 = 0.17$, the ideal gain $10\log_{10}(\gamma_1 + \gamma_2) = 0.68$ dB. The degradation to the ideal gain versus the 70-m symbol SNR ($E_{s1}/N_{01}$) is shown in Fig. 8 for a symbol rate of 200 sps and a modulation index of 70 deg. In Fig. 8, the degradation for the end-to-end system in Fig. 3 is shown by the solid line and obtained by evaluating Eq. (23). The degradation due to the individual components is shown by the broken lines. For example, the degradation due to the carrier loop, shown by the top line (CA) in Fig. 8 is found by assuming that all the other components in the array have ideal operation, that is, by evaluating Eq. (23) as follows:

$$D|_{[SNR_{n1}=\rho_{sc}=\rho_{sy}=\infty]} = 10\log_{10}\overline{C_c^2} \tag{42}$$

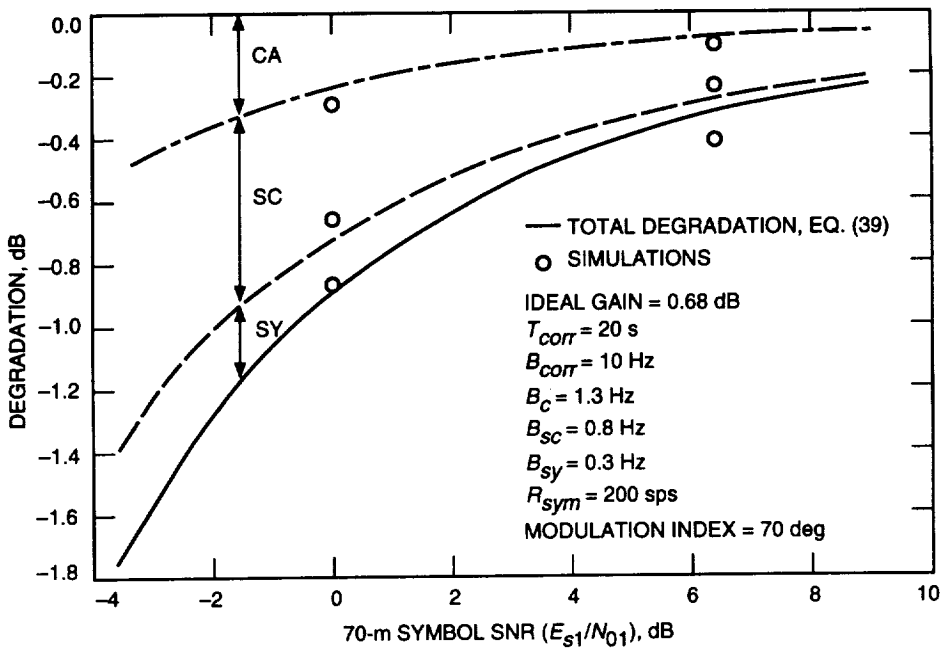


**Fig. 8. SSNR degradation for an array of two different antennas.**

The second line from the top (SC) is the degradation due to the carrier and subcarrier, and the bottom line (SY) is the carrier, subcarrier, and symbol or total degradation. The IF carrier combining and baseband telemetry combining degradations are not shown individually because they are negligible. Note that it was shown in [1] that the total degradation in dB is approximately equal to the sum of the individual degradations. Results obtained by simulating the system in Fig. 3 are indicated by the circles.

SER curves needed to compute the loss are shown in Fig. 9. The bottom curve is the SER assuming an array with ideal gain (0.68 dB). The SER for nonideal gain, Eq. (40), is shown by the curve in the middle. Simulation results for a nonideal array are shown as circles. At the top is the nonideal performance for a single 70-m antenna, Eq. (19). In the example, the conditional SNR, $P_s'(E)$ in Eq. (40), is given by Eq. (41) with

$$C_{comb} = \frac{\gamma_1^2 + \gamma_2^2}{\gamma_1 + \gamma_2} + \frac{2\gamma_1\gamma_2}{\gamma_1 + \gamma_2} \cos(\Delta\phi_{21}) \tag{43}$$

where $\gamma_1 = 1$ and $\gamma_2 = 0.17$.

The degradation and loss for various SERs are given in Table 2. The second column in the table is the symbol SNR needed (at antenna 1) for an ideal array to achieve the SER in column 1. The loss in the third column is the additional SNR needed by a nonideal system to achieve the same SER as an ideal one. For example, to achieve an SER of $10^{-2}$, an ideal array requires that $E_{s1}/N_{01} = 3.7$ dB, whereas a practical system would require that $E_{s1}/N_{01} = (3.7 + 0.5)$ dB. The degradation in the fourth column is the reduction in the ideal SNR gain observed at the matched filter output. For instance, in our two-antenna example, since the symbol SNR at the 70-m antenna is ideally equal to 3.7 dB, then the observed or measured combined symbol SNR would be $(3.7 + 0.68 - 0.5)$ dB.

**2. Array of Four 34-m Antennas.** Analytical and simulation results for the symbol SNR degradation of an array of four 34-m STD antennas (i.e., $L = 4$ in Fig. 3) are shown in Fig. 10. In this

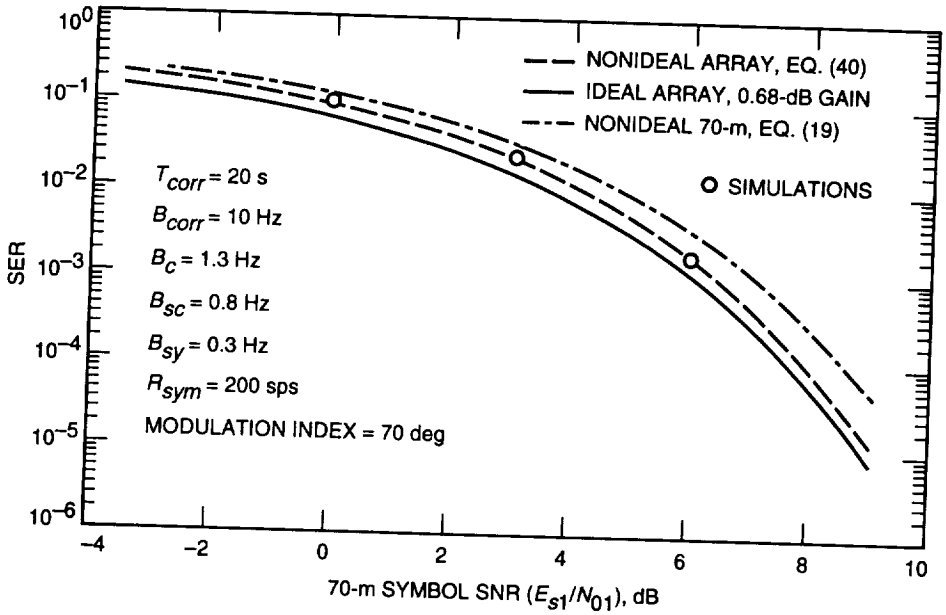


**Fig. 9. SER for an array of two different antennas.**

**Table 2. SNR loss versus SSNR degradation (array of one 34-m STD and one 70-m antenna).**

| SER | $E_{s1}/N_{01}$ | Loss, dB | Degradation, dB |
|---|---|---|---|
| $10^{-1}$ | −1.5 | −1.3 | −1.2 |
| $10^{-2}$ | 3.7 | −0.5 | −0.5 |
| $10^{-3}$ | 6.1 | −0.4 | −0.4 |
| $10^{-4}$ | 7.7 | −0.3 | −0.3 |

case, because all the antennas have the same efficiency and aperture, $\gamma_i = 1$ for all $i$. The analytical degradation is computed as before, using Eq. (39) with $C_{comb}$ given by Eq. (38) as follows:

$$C_{comb} = 1 + \frac{1}{2}[\cos(\Delta\phi_{21}) + \cos(\Delta\phi_{31}) + \cos(\Delta\phi_{41}) + \cos(\Delta\phi_{31} - \Delta\phi_{21}) + \cos(\Delta\phi_{41} - \Delta\phi_{21}) + \cos(\Delta\phi_{41} - \Delta\phi_{31})] \quad (44)$$

SER for this example is shown in Fig. 11. Curves are obtained for an array with ideal gain ($10\log_{10}(4) =$ 6 dB), nonideal gain [Eq. (40)], and a single receiver with nonideal synchronization [Eq. (19)]. Degradation and loss for various SER values are tabulated in Table 3.

## IV. Carrier Aiding

In carrier aiding, the "master antenna" is assumed to lock on the carrier and, subsequently, rate aid the other antennas. As shown in Fig. 2, the received signal at antenna $i = (2, \cdots, L)$ is first downconverted using the carrier reference from the master antenna and then tracked using a baseband PLL. If we assume that all the elements in the array are colocated, the $i$th PLL can operate at much narrower bandwidths

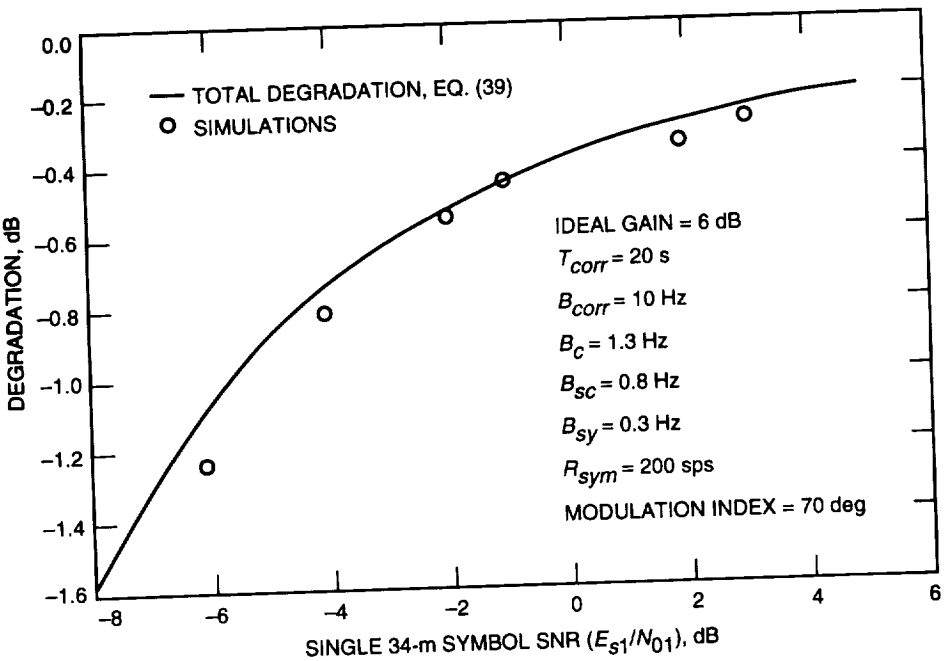


**Fig. 10. SSNR degradation for an array of four identical antennas.**

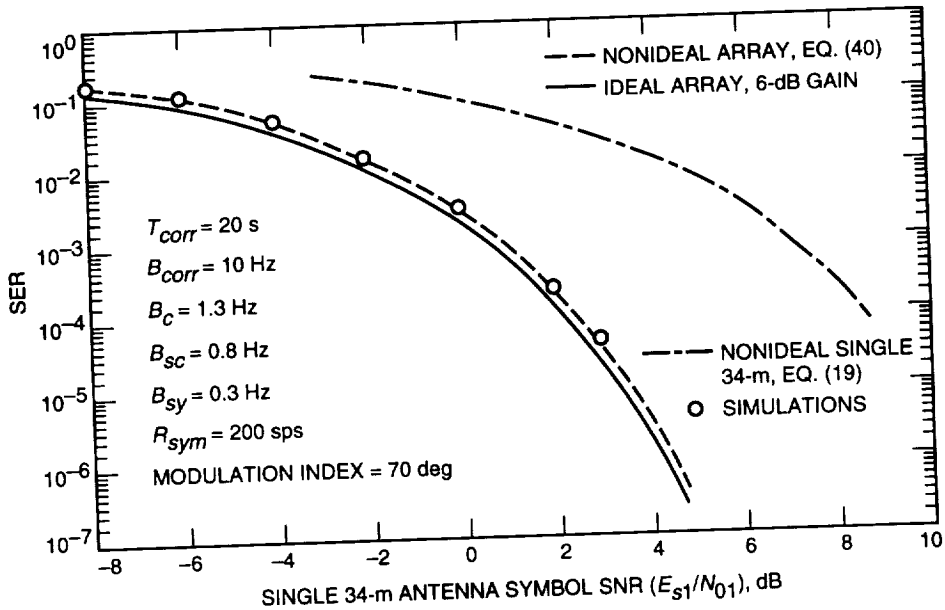


**Fig. 11. SER for an array of four identical antennas.**

than in the absence of rate aiding, because it need only track the Doppler dynamics relative to the master antenna. After carrier demodulation, the signals from each antenna are sent to a central location where they are time delayed, weighted, combined, and then passed through a chain of subcarrier loop, symbol loop, and matched filter. Degradation and loss for this scheme are derived as before. However, now the degradation and loss are a function of the phase error of $L$ carrier loops. Two quantities that are needed to derive the performance of this system are the loop SNR of the $i$th carrier loop, $\rho_{c_i}$, and the joint probability density function of the carrier phase errors $\phi_{\mathbf{c}} = (\phi_{c_1}, \phi_{c_2}, \cdots, \phi_{c_L})$.

**Table 3. SNR loss versus SSNR degradation (array of four 34-m STD antennas).**

| SER | $E_{s1}/N_{01}$ | Loss, dB | Degradation, dB |
|---|---|---|---|
| $10^{-1}$ | −6.9 | −1.3 | −1.3 |
| $10^{-2}$ | −1.7 | −0.5 | −0.5 |
| $10^{-3}$ | 0.77 | −0.4 | −0.4 |
| $10^{-4}$ | 2.4 | −0.35 | −0.3 |

## A. Derivations of $\rho_{c_i}$ and Joint Probability Density Function of $\phi_c$

Since the operation of the master PLL in Fig. 2 is unaffected by the PLLs at the other antennas, its loop SNR, $\rho_{c_1}$, is given by Eq. (8). The aided loop, on the other hand, is directly affected by the performance of the master PLL, so its loop SNR can be expected to be related to the loop SNR (and bandwidth) of the master antenna. For residual and suppressed-carrier modulation, the aided-loop loop SNR, denoted $\rho_{c_i}$, is shown in the Appendix, using Fokker–Planck, to be

$$\rho_{c_i} = \left[\frac{1}{\rho'_{c_i}} + \frac{\xi_{1i}}{3\rho_{c_1}} \frac{2 + 4\xi_{1i} + 5\xi_{1i}^2 + 3\xi_{1i}^3}{1 + 2(\xi_{1i} + \xi_{1i}^2 + \xi_{1i}^3) + \xi_{1i}^4}\right]^{-1} \tag{45}$$

where, for residual carrier modulation, $\rho'_{c_i} = (P_{C_i}/N_{0i})/B_{c_i}$, and, for suppressed-carrier modulation, $\rho'_{c_i} = (P_{D_i}/N_{0i})/B_{c_i}\,(1 + (1/2E_{s_i}/N_{0_i}))^{-1}$. The parameter $\xi_{1i}$ denotes the ratio of the loop bandwidth and is given by

$$\xi_{1i} = \frac{B_{c_1}}{B_{c_i}} \tag{46}$$

Some insight into the last equation can be given by examining the relationship between the master and aided loops in the following four cases: (1) $B_{c_i} \to \infty$, $B_{c_1}$ fixed, (2) $B_{c_1} \to 0$, $B_{c_i}$ fixed, (3) $B_{c_i} \to 0$, $B_{c_1}$ fixed, and (4) $B_{c_1} \to \infty$, $B_{c_i}$ fixed. Note that cases (3) and (4) are of most interest because, in practice, $B_{c_i} \ll B_{c_1}$ and, equivalently, $\xi_{1i} \gg 1$.

Case (1): In the limit $B_{c_i} \to \infty$, the loop SNR $\rho_{c_i} \to 0$, as expected. Case (2): Recall that in our model of the IF signals [see Eq. (24)], the phase at antenna $i$ is given by $\theta_i = \theta_1 + \Delta\theta_{i1}$, where $\theta_1$ is the phase of the master antenna and $\Delta\theta_{i1}$ is the phase at antenna $i$ relative to antenna 1. If the master loop is tracking, the phase input to the $i$th loop is $\phi_{c_1} + \Delta\theta_{i1}$, where $\phi_{c_1}$ is the tracking error at antenna 1. Now suppose that the master loop is tracking $\theta_1$ perfectly (i.e, $\phi_{c_1} \to 0$, or alternatively, $\rho_{c_1} \to \infty$ and $B_{c_1} \to 0$); then intuitively we can expect the master loop not to degrade the tracking performance of the aided loop. Letting $B_{c_1} \to 0$ in Eq. (45), we find that $\rho_{c_i} \to \rho'_{c_i}$, which is independent of $\rho_{c_1}$. Case (3): As $B_{c_i} \to 0$, $\rho_{c_i} \to \rho_{c_1}$, as shown in Fig. 12 for the case of a 70-m and a 34-m antenna. The broken line in the figure is obtained by evaluating Eq. (45), whereas the circles represent simulation results for two PLLs in cascade. One way to view this result is by letting the received phase at both antennas be the same (i.e., $\Delta\theta_{i1} = 0$ for $i \neq 1$). Then, the input to the second loop is the noise process $\phi_{c_1}$. Intuitively, we would not expect the second loop to be able to reduce the phase error or noise from the first loop. Hence, it seems reasonable that even for loop bandwidths approaching zero, the loop SNR of the $i$th loop can never be greater than $\rho_{c_1}$. Case (4): The limit $B_{c_1} \to \infty$ implies that loop 1 is not tracking the carrier

and, therefore, the signal into the cascaded loop is one mixed by an incoherent reference. Hence, in this case, we can expect the cascaded loop not to track its input either. The inability of the cascaded loop to track the signal is shown in Fig. 13, where, in the limit, $\rho_{c_2}$ approaches zero. From the above cases, we can conclude that $\rho_{c_i} \leq \rho_{c_1}$.

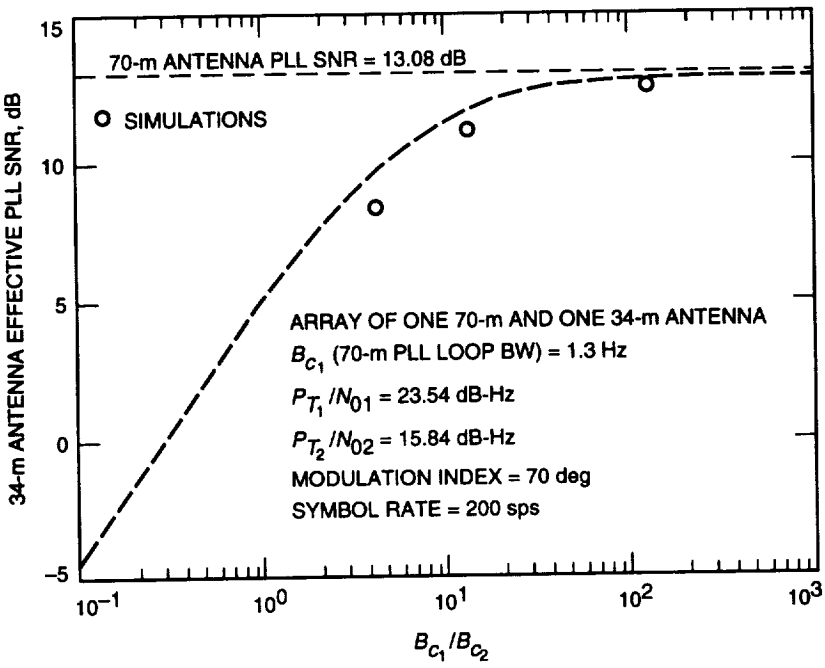


**Fig. 12. Loop SNR limit case (3).**

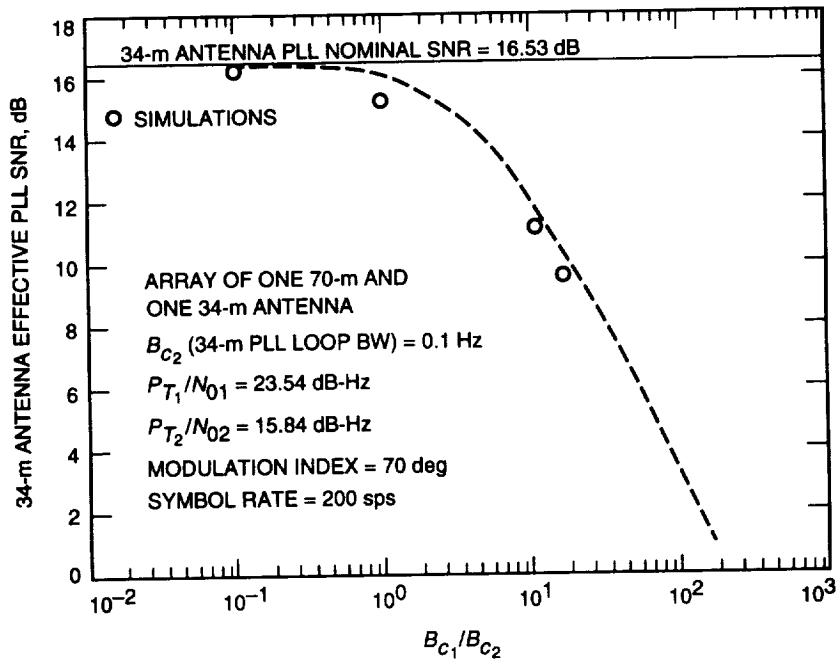


**Fig. 13. Loop SNR limit case (4).**

Next we turn to the derivation of $p(\phi_{c_1}, \phi_{c_2}, \cdots, \phi_{c_L})$, which is needed to determine the SER and loss. We begin with the derivation of $p(\phi_{c_i}, \phi_{c_1})$. Note that, from $\theta_i = \theta_1 + \Delta\theta_{i1}$, it is clear that for $i \neq 1$, $\theta_i$ and $\theta_1$ are not independent. Assuming that $p(\phi_{c_1})$ is Thikonov distributed as in Eq. (7), the joint density $p(\phi_i, \phi_1)$ is derived in the Appendix to be

$$p(\phi_{c_1}, \phi_{c_i}) = \begin{cases} \dfrac{\exp\left[\alpha_i \cos\left(\phi_{c_i} - \eta_{1i}\sqrt{\rho_{c_1}/\rho_{c_i}}\phi_{c_1}\right) + \rho_{c_1}\cos(\phi_{c_1})\right]}{(2\pi)^2 I_0(\alpha_i) I_0(\rho_{c_1})} & \text{residual-carrier case} \\ \dfrac{\exp\left[(\alpha_i/4)\cos\left[2\left(\phi_{c_i} - \eta_{1i}\sqrt{\rho_{c_1}/\rho_{c_i}}\phi_{c_1}\right)\right] + (\rho_{c_1}/4)\cos(2\phi_{c_1})\right]}{(\pi)^2 I_0(\alpha_i/4) I_0(\rho_{c_1}/4)} & \text{suppressed-carrier case} \end{cases} \tag{47}$$

where $\alpha_i = \rho_{c_i}/(1 - \eta_{1i}^2)$, and where the correlation coefficient, $\eta_{1i}$, is shown in the Appendix to be

$$\eta_{1i} = \sqrt{\frac{\rho_{c_i}}{\rho_{c_1}}}\left[\frac{\xi_{1i}^2}{3}\,\frac{1 + 4\xi_{1i} + 3\xi_{1i}^2}{1 + 2(\xi_{1i} + \xi_{1i}^2 + \xi_{1i}^3) + \xi_{1i}^4}\right] \tag{48}$$

Some insight into Eq. (47) can be given by once again considering the extreme cases when $B_{c_i} \to 0$ and $B_{c_i} \to \infty$. We have already seen that when $B_{c_1}$ is fixed and $B_{c_i} \to \infty$, then $\rho_{c_i} \to 0$. Hence, in this limit, the loop is unable to track, and we can expect $p(\phi_{c_i})$ to be uniformly distributed in the interval $[-\pi, \pi]$ for the residual-carrier case and in the interval $[-(\pi/2), \pi/2]$ for the suppressed-carrier case, respectively. It can be shown that

$$\begin{aligned} p(\phi_{c_i})|_{B_{c_i}=\infty} &= \lim_{B_{c_i}\to\infty} \int_{\phi_{c_1}} p(\phi_{c_1}, \phi_{c_i}) d\phi_{c_1} \\ &= \begin{cases} \dfrac{1}{2\pi} & \text{residual-carrier case} \\ \dfrac{1}{\pi} & \text{suppressed-carrier case} \end{cases} \end{aligned} \tag{49}$$

for both cases in Eq. (47). Similarly, it can be shown that when $B_{c_1}$ is fixed and $B_{c_i} \to 0$, the density is given as

$$\begin{aligned} p(\phi_{c_i})|_{B_{c_i}=0} &= \lim_{B_{c_i}\to 0} \int_{\phi_{c_1}} p(\phi_{c_1}, \phi_{c_i}) d\phi_{c_1} \\ &= \begin{cases} \dfrac{\exp[\rho_{c_1}\cos(\phi_{c_i})]}{2\pi I_0(\rho_{c_1})} & \text{residual-carrier case} \\ \dfrac{\exp[(\rho_{c_1}/4)\cos(2\phi_{c_i})]}{\pi I_0(\rho_{c_1}/4)} & \text{suppressed-carrier case} \end{cases} \end{aligned} \tag{50}$$

Notice that the last equation is a function of the master-loop loop SNR $\rho_{c_1}$, not $\rho_{c_i}$. This is consistent with our earlier result, where we concluded that the upper limit of the aided-loop loop SNR (i.e., as $B_{ci} \to 0$) is equal to $\rho_{c_1}$.

The joint probability density function (pdf) $p(\phi_{c_1}, \phi_{c_2}, \cdots, \phi_{c_L})$ is found by applying Bayes Theorem, namely,

$$\begin{aligned} p(\phi_{c_1}, \phi_{c_2}, \cdots, \phi_{c_L}) &= p(\phi_{c_2}, \cdots, \phi_{c_L}|\phi_{c_1})p(\phi_{c_1}) \\ &= p(\phi_{c_1})p(\phi_{c_2}|\phi_{c_1})p(\phi_{c_3}|\phi_{c_1}) \cdots p(\phi_{c_L}|\phi_{c_1}) \\ &= p(\phi_{c_1}) \prod_{i=2}^{L} \left[ \frac{p(\phi_{c_1}, \phi_{c_i})}{p(\phi_{c_1})} \right] \end{aligned} \tag{51}$$

where $p(\phi_{c_1})$ and $p(\phi_{c_1}, \phi_{c_i})$ are given by Eqs. (7) and (47), respectively. The last equation simplifies to its final form because $p(\phi_{c_i}/\phi_{c_1})$ and $p(\phi_{c_j}/\phi_{c_1})$ are independent for $i \neq j$.

One more quantity needed to describe the performance of carrier aiding is the joint pdf of $\phi_m$ and $\phi_n$ for $m \neq n$ and $m, n \neq 1$. We start with the identity

$$p(\phi_{c_m}, \phi_{c_n}) = \int_{\phi_{c_1}} p(\phi_{c_1}, \phi_{c_m}, \phi_{c_n}) d\phi_{c_1} \tag{52}$$

Using Eq. (51) for $p(\phi_{c_1}, \phi_{c_m}, \phi_{c_n})$, we have

$$p(\phi_{c_m}, \phi_{c_n}) = \int_{\phi_{c_1}} \frac{p(\phi_{c_1}, \phi_{c_m}) p(\phi_{c_1}, \phi_{c_n})}{p(\phi_{c_1})} d\phi_{c_1} \tag{53}$$

### B. Performance of Carrier Aiding

Assuming as before that the time delay for each antenna is perfectly estimated, then following the same steps as in [1,2], the samples of the combined signal at the output of the matched filter are given by

$$v_k = \begin{cases} \sqrt{P_{D_1}} \left( \sum_{i=1}^{L} \gamma_i C_{c_i} \right) C_{sc} d_k + n_k & d_k = d_{k-1} \\ \sqrt{P_{D_1}} \left( \sum_{i=1}^{L} \gamma_i C_{c_i} \right) C_{sc} \left( 1 - \frac{|\phi_{sy}|}{\pi} \right) d_k + n_k & d_k \neq d_{k-1} \end{cases} \tag{54}$$

where $C_{c_i} = \cos(\phi_{c_i})$, and all other terms are as defined earlier. The symbol SNR conditioned on $\phi_{c_i}$, $\phi_{sc}$, and $\phi_{sy}$ is given from Eq. (12) as

$$SSNR' = \begin{cases} \frac{2P_{D_1}T}{N_{01}} C_{comb} C_{sc}^2 & d_k = d_{k-1} \\ \frac{2P_{D_1}T}{N_{01}} C_{comb} C_{sc}^2 \left( 1 - \frac{|\phi_{sy}|}{\pi} \right)^2 & d_k \neq d_{k-1} \end{cases} \tag{55}$$

where

$$C_{comb} = \frac{\left[ \sum_{i=1}^{L} \gamma_i C_{c_i} \right]^2}{\sum_{i=1}^{L} \gamma_i} \tag{56}$$

**1. Degradation.** Proceeding as in Section III, the SSNR degradation for this case is determined by averaging Eq. (55) over all the phase errors and then dividing the result with the ideal combined SNR. Hence,

$$D = 10\log_{10}\left[\overline{C_{sc}^2 C_{sy}^2}\left(\frac{\sum_{m=1}^{L}\gamma_m^2\overline{C_{c_m}^2} + \sum_{m=1}^{L}\sum_{\substack{n=1\\n\neq m}}^{L}\gamma_m\gamma_n\overline{C_{c_m,c_n}}}{(\sum_{m=1}^{L}\gamma_m)^2}\right)\right] \tag{57}$$

where $\overline{C_{c_m}^2}$ is given by using the appropriate loop SNR in Eq. (15), and $\overline{C_{sc}^2}$ and $\overline{C_{sy}^2}$ are as defined earlier. The first moment of the joint carrier degradation, $\overline{C_{c_m,c_n}}$, is defined as

$$\overline{C_{c_m,c_n}} = \int_{\phi_{c_n}}\int_{\phi_{c_m}} \cos(\phi_{c_m})\cos(\phi_{c_n})p(\phi_{c_m},\phi_{c_n})d\phi_{c_m}d\phi_{c_n} \tag{58}$$

After substituting Eq. (53) for the joint pdf, we have the following equation that must be computed numerically:

$$\overline{C_{c_m,c_n}} = \int_{\phi_{c_n}}\int_{\phi_{c_m}}\int_{\phi_{c_1}} \cos(\phi_{c_m})\cos(\phi_{c_n})\left[\frac{p(\phi_{c_1},\phi_{c_m})p(\phi_{c_1},\phi_{c_n})}{p(\phi_{c_1})}\right]d\phi_{c_1}d\phi_{c_m}d\phi_{c_n} \tag{59}$$

Ideally, when there are no phase errors (i.e., when $\rho_{c_i} = \rho_{sc} = \rho_{sy} = \infty$), $\overline{C_{c_m}^2} = \overline{C_{c_m,c_n}} = \overline{C_{sc}^2} = \overline{C_{sy}^2} = 1$ and Eq. (57) becomes zero, as expected.

**2. Loss.** The carrier-aiding SER for an $L$ antenna array is defined as

$$P_s(E) = \int_{\phi_{sc}}\int_{\phi_{sy}}\int_{\phi_{c_1}}\int_{\phi_{c_2}}\cdots\int_{\phi_{c_L}} P_s'(E)\times[p(\phi_{sc})p(\phi_{sy})\times p(\phi_{c_1},\phi_{c_i},\cdots,\phi_{c_L})]\,\mathbf{d}\phi_{\mathbf{c}}d\phi_{sy}d\phi_{sc} \tag{60}$$

where $\mathbf{d}\phi_{\mathbf{c}} = d\phi_{c_1}d\phi_{c_2}\cdots d\phi_{c_L}$. The conditional SER, $P_s'(E)$, is obtained by substituting Eq. (55) in Eq. (20). After some algebra, we have

$$P_s'(E) = \frac{1}{4}\text{erfc}\left[\sqrt{\frac{E_{s1}}{N_{01}}C_{comb}}C_{sc}\left(1-\frac{|\phi_{sy}|}{\pi}\right)\right] + \frac{1}{4}\text{ erfc}\left[\sqrt{\frac{E_{s1}}{N_{01}}C_{comb}}C_{sc}\right] \tag{61}$$

where $E_{s1}/N_{01} = P_{D_1}T/N_{01}$ is the symbol SNR at the "master" antenna and $C_{comb}$ was defined earlier in Eq. (56). Again, as a check, we note that, when there are no timing errors, Eq. (61) reduces to the well known BPSK error rate for an ideal array of $L$ antennas, namely, $P_s(E) = 1/2$ erfc $(\sqrt{\sum_{i=1}^{L}(E_{si}/N_{0i})})$.

### C. Example: Array of One 70-m and One 34-m Antenna

The degradation and loss for carrier aiding using residual carrier and suppressed-carrier modulation are presented here for a two-element array of one 70-m antenna and one STD 34-m antenna. As in the carrier-arraying with a single PLL case, the 70-m antenna is chosen as the reference antenna so $\gamma_1 = 1$ and $\gamma_2 = 0.17$. Furthermore, the symbol rate is 200 sps, and the modulation index for the residual carrier case is 70 deg.

The analytical results for residual carrier modulation are obtained by using the PLL loop SNR in Eqs. (57) and (60), whereas the results for the suppressed case use the same equations with the Costas loop SNR instead. The analytical [Eq. (57)] and simulated degradation results for residual and suppressed-carrier modulation are shown in Figs. 14 and 15, respectively. The individual degradations due to the carrier (CA), subcarrier (SC), and symbol (SY) tracking error are shown by the broken lines. As before, the individual degradations are obtained by using infinite loop SNR in Eq. (57) for all the loops except the one whose degradation contribution is desired.

The SER performance for the residual case is depicted in Fig. 16 and in Fig. 17 for the suppressed case. In both figures, the curves shown are for an array with an ideal gain of 0.68 dB; an array with nonideal gain, Eq. (60); and the nonideal performance of a single 70-m antenna, Eq. (19). Simulated SER results for the nonideal array are shown as circles. Note that the conditional SER in Eq. (60) for this example is given as

$$P_s'(E) = \frac{1}{4}\left[\operatorname{erfc}\left[\sqrt{\frac{E_{s1}}{N_{01}}\frac{(C_{c_1}+\gamma_2 C_{c_2})^2}{\gamma_1+\gamma_2}C_{sc}}\left(1-\frac{|\phi_{sy}|}{\pi}\right)\right] + \operatorname{erfc}\left[\sqrt{\frac{E_{s1}}{N_{01}}\frac{(C_{c_1}+\gamma_2 C_{c_2})^2}{\gamma_1+\gamma_2}C_{sc}}\right]\right] \quad (62)$$

For the residual carrier case, degradation and loss at specific SER values are shown in Table 4.

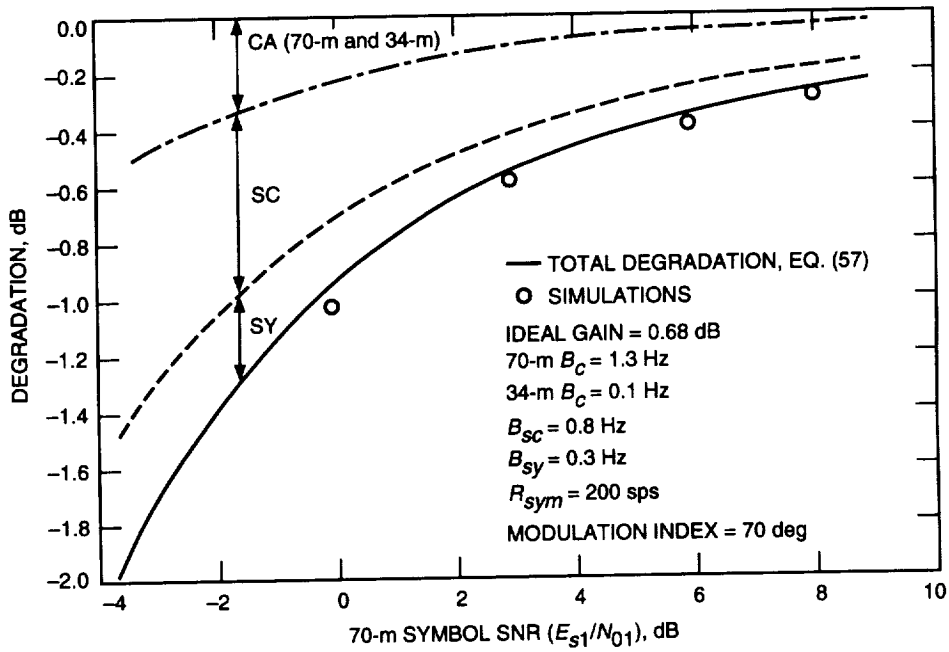


**Fig. 14. SSNR degradation for an array of two different antennas (CA-aid).**

## V. Carrier Arraying Using Multiple Carrier Loops

Carrier arraying using multiple carrier loops is shown in Fig. 4. As explained earlier, this scheme is an improvement over carrier aiding because feedback from the aided loops enables the master loop to operate at a higher loop SNR than in the absence of feedback. The disadvantage of this scheme is that, for the array to get started, at least one of the antennas seems to require to lock on the carrier. For residual carrier modulation, this technique has been partially analyzed [12,13] and also demonstrated [13]. In [12], analytical expressions for the phase error variance (due to thermal noise) of the master loop, as

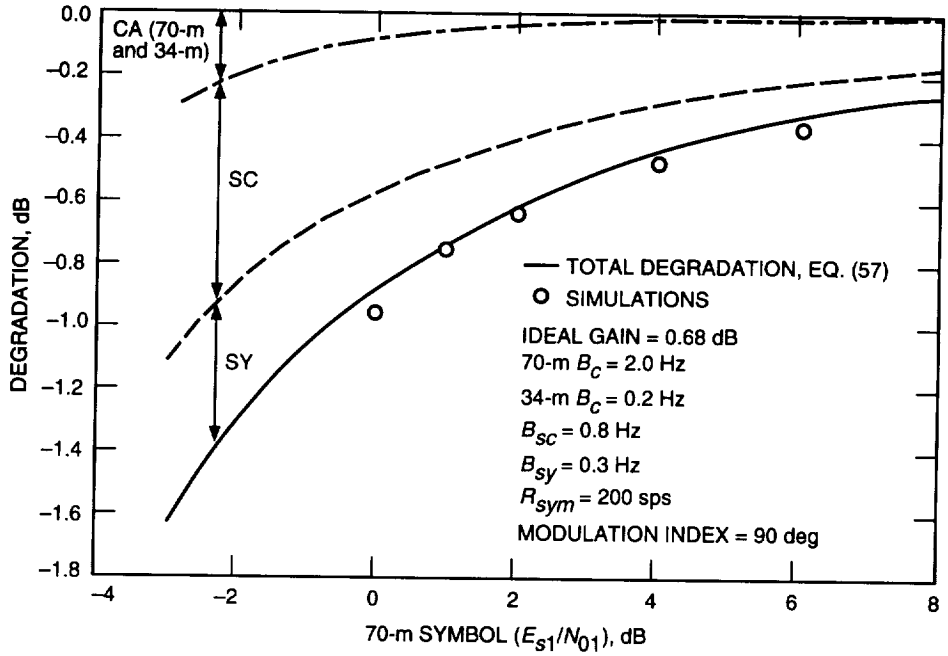


**Fig. 15. SSNR degradation for an array of two different antennas, suppressed carriers (CA-aid).**

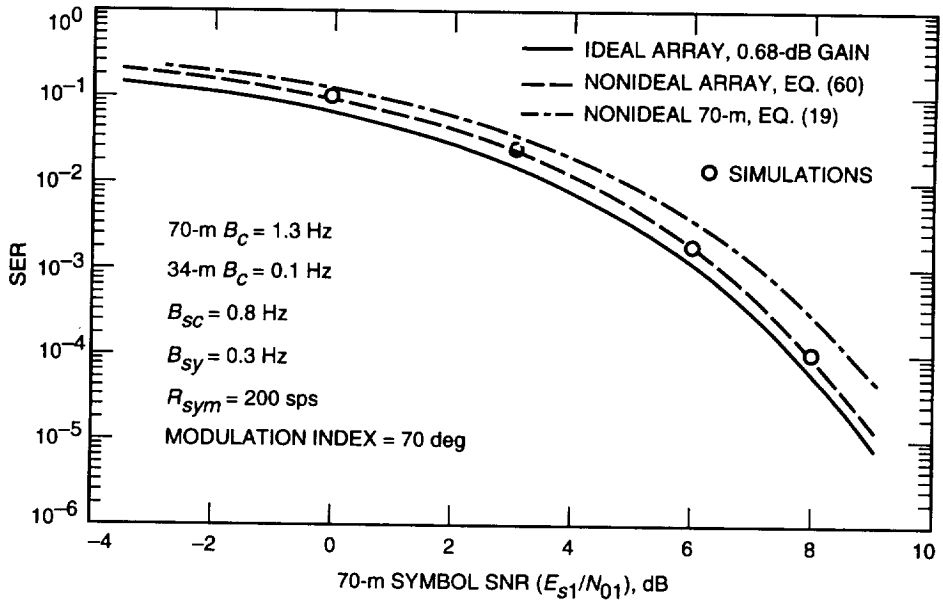


**Fig. 16. SER for an array of two different antennas (CA-aid).**

well as the aided (slave) loops, were presented. An extension of this theory that included the effects of oscillator phase noise on loop jitter was given in [13]. Analytical expressions for degradation and loss for the end-to-end system have yet to be presented. In our study, we obtained results for the degradation and loss by simulating Fig. 6. We would like to note that we were not able to match certain intermediate simulation results with the theory presented in [12]. Specifically, we found that the loop SNR of the aided loop obtained via simulations differed substantially from the theory presented in [12]. The cause of this discrepancy, we believe, is due to neglecting all the terms (including first-order terms) involving the carrier loop bandwidth ratio, $B_{c_i}/B_{c_1}$, in evaluating the integral [12, Eq. (60)].

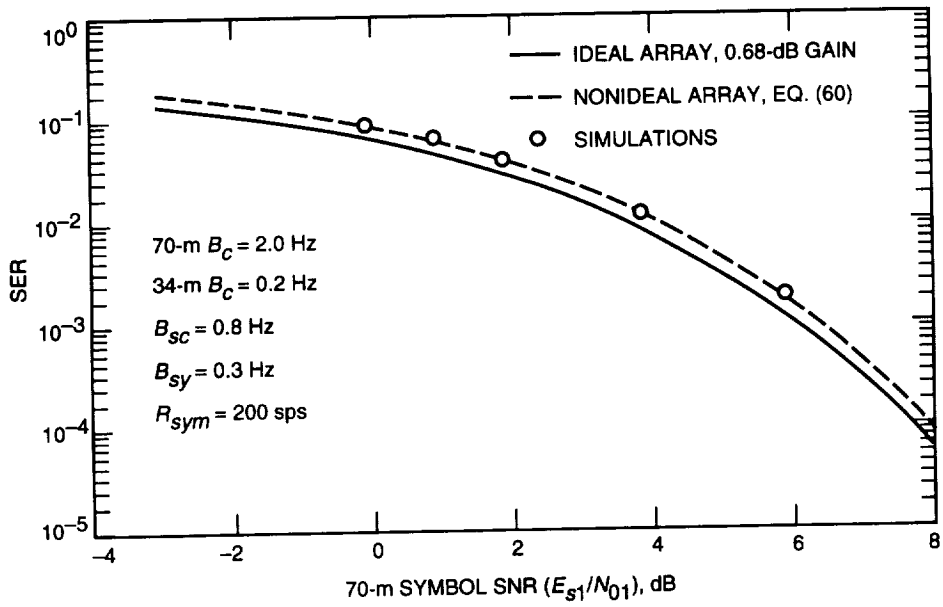


**Fig. 17. SER for an array of two different antennas, suppressed carrier (CA-aid).**

**Table 4. SNR loss versus SSNR degradation (carrier aiding: array of one 34-m STD and one 70-m antenna).**

| SER | $E_{s1}/N_{01}$ | Loss, dB | Degradation, dB |
|---|---|---|---|
| $10^{-1}$ | −1.5 | −1.4 | −1.3 |
| $10^{-2}$ | 3.7 | −0.6 | −0.5 |
| $10^{-3}$ | 6.1 | −0.4 | −0.4 |
| $10^{-4}$ | 7.7 | −0.3 | −0.3 |

The deviation between the existing theory for residual carrier modulation and our simulation results is illustrated using an array of one 34-m high efficiency (HEF) antenna and one 34-m STD antenna operating at S-band. Let the 34-m STD be the master antenna; then, from Table 1, $\gamma_1 = 1$ and $\gamma_2 = 0.07/0.17 = 0.41$. The ideal gain is $10\log_{10}(\gamma_1 + \gamma_2) = 1.5$ dB. For simulation purposes, we set $(P_C/N_0)_{STD} = 10$ dB-Hz, $(P_C/N_0)_{HEF} = 6.1$ dB-Hz, and $B_{c,STD} = 1$ Hz. Hence, without arraying, the master-PLL loop SNR is 10 dB. The master-PLL loop SNR in the arrayed system, denoted $\rho_{c,STD}$, should be higher than 10 dB, due to error signal feedback from the aided loop. Note that the improvement in the master-PLL loop SNR, which is maximum when the error signals add coherently, can be expected to be an upper bound on the ideal arraying gain $(1 + \gamma_2)$, or 1.5 dB. The loop SNR, $\rho_{c,STD}$, is shown in Fig. 18 as a function of the ratio between the master loop bandwidth and the aided-loop bandwidth, $B_{c,HEF}$. The bottom solid line in Fig. 18 is the loop SNR of the master loop predicted by the analysis in [12]; applying our example to the result in [12, Eq. (26)] yields

$$\rho_{STD} = \frac{1}{\sigma^2_{\phi_{c1}}} = \frac{3\rho'_{STD}\delta}{\lambda} \tag{63}$$

where $\rho'_{STD} = ((P_C/N_o)_{STD})/B_{c,STD} = 10$ dB is the nominal master loop SNR, and

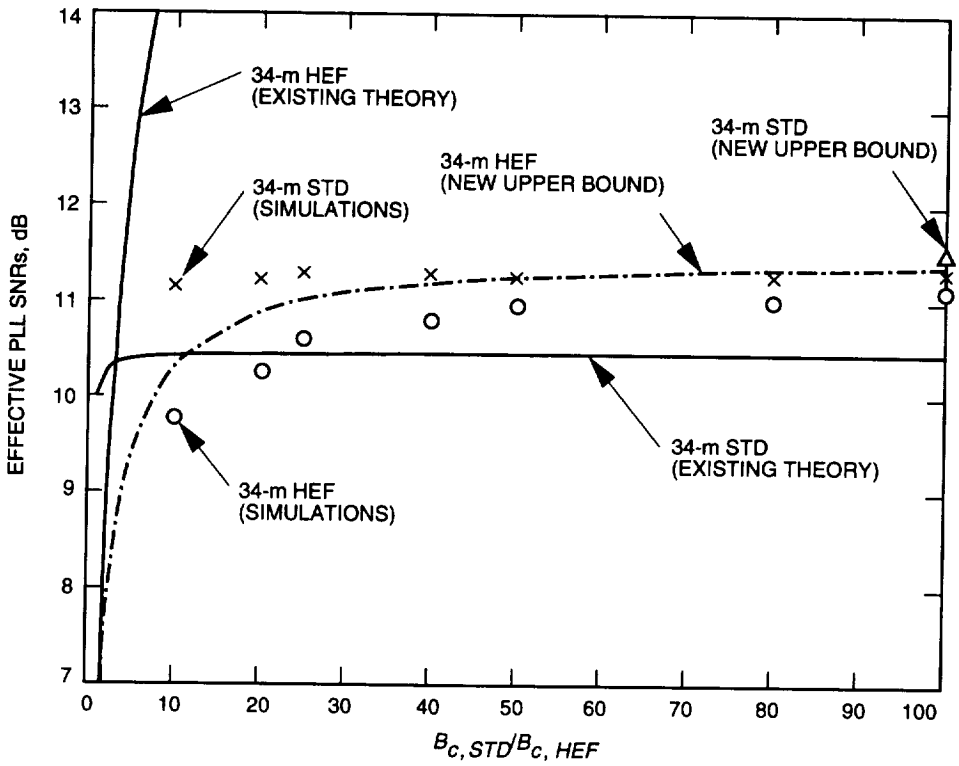


**Fig. 18. Effective loop SNRs.**

$$\lambda = 4G(1+2G) + 4G(5+G)\xi + 4(7G-1)\xi^2 + 4(1+5G)\xi^3 + 12\xi^4 \tag{64}$$

$$\delta = 4G^2 + 4(3G-1)\xi + 8G\xi^2 + 4(1+G)\xi^3 + 4\xi^4 \tag{65}$$

where $\xi = B_{c,HEF}/B_{c,STD}$, and $G = \gamma_1 + \gamma_2$ is the ideal gain. Note that the above expressions are for a carrier loop with a second-order loop filter with the damping parameter $r = 2$. The maximum gain or improvement predicted by Eq. (63) can be found by keeping $B_{c,STD}$ fixed and letting $B_{c,HEF} \to 0$. For the example given, the upper limit of the master PLL loop SNR is the value $\rho|_{B_{c,HEF}=0}$, shown in Fig. 18. Hence, the theory seems to predict that the maximum improvement is less than the ideal arraying gain. Notice in Fig. 18 that as $B_{c,HEF} \to 0$, the simulated loop SNR (shown as $\times$) approaches the maximum achievable loop SNR of (10 + 1.5) dB, denoted by $\Delta$ in the figure. Next we turn to the aided-PLL SNR, $\rho_{HEF}$, which is also shown in Fig. 18 versus $B_{c,STD}/B_{c,HEF}$. The aided-loop SNR as predicted by [12, Eq. (61)], namely,

$$\rho_{HEF} = \frac{1}{\sigma^2_{\phi_{c_2}}} = \left\{ \frac{\xi}{3\,G\,\rho'_{STD}} \left[ G + 2 + \frac{\gamma_2(4G+10)}{G^2+2G+5} \right] + \frac{1}{\rho'_{HEF}} \left[ 1 - \frac{2\gamma_2(3G+5)}{3(G^2+2G+5)} \right] \right\}^{-1} \tag{66}$$

is shown by the top solid line in Fig. 18. The quantity $\rho'_{HEF}$ in Eq. (66) is the nominal carrier loop SNR of the aided antenna and is equal to $((P_C/N_o)_{HEF})/B_{c,HEF}$. Keeping $B_{c,STD}$ fixed, and letting $B_{c,HEF} \to 0$, we find that $\rho_{HEF} \to \infty$, whereas the simulated results (shown as circles) approach the master-loop SNR. The simulation results for the aided loop are consistent with the theory and results

for the carrier-aiding scheme in Fig. 2. Recall that in Section III we concluded that the loop SNR of the aided loop is upper bounded by that of the master loop. Interestingly, if we assume that there is perfect feedback from the aided loop so that the master loop is operating with a 1.5-dB improvement, then using Eq. (45), we can determine the upper bound on the second loop SNR, which is represented by (-·-) in Fig. 18.

### A. Example: Simulating an Array of One 70-m and One 34-m Antenna

As in the two previous schemes, we present the degradation and loss for a two-element array of one 70-m and one STD 34-m antenna. The results are obtained by simulations. For comparison purposes, we use the same exact parameters used before. The symbol SNR degradation results are shown in Fig. 19, and the SER performance is presented in Fig. 20. It is observed that the degradation and loss results are better than the carrier aiding and worse than the carrier-array with a single PLL example.

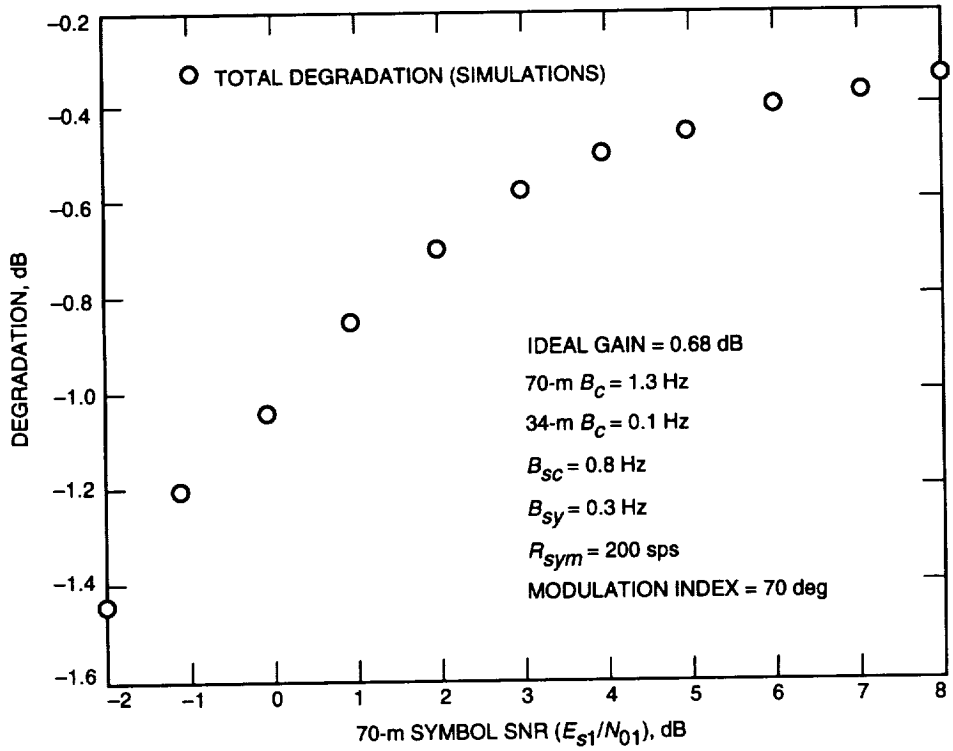


**Fig. 19. Degradation (simulations).**

## VI. Conclusion

Three similar techniques that use carrier information from multiple antennas to enhance carrier acquisition and tracking were presented in conjunction with baseband combining. It was shown that the carrier arraying using a single carrier loop technique can acquire and track the carrier, even when any single antenna in the array cannot do so by itself. The carrier aiding and carrier arraying using multiple carrier loops techniques, on the other hand, were shown to lock the carrier only when one of the array elements has sufficient margin to acquire the carrier on its own. The tracking performance of these techniques was shown to be almost equal for medium and high data rates. For low data rates, however, carrier arraying using a single PLL has the best performance, followed by carrier arraying using multiple PLLs, and then carrier aiding.

The analytical expressions for degradation and loss of the carrier arraying using a single PLL and the carrier aiding schemes were confirmed by simulations of the end-to-end system. The carrier arraying using multiple carrier loops technique was evaluated by simulation alone.

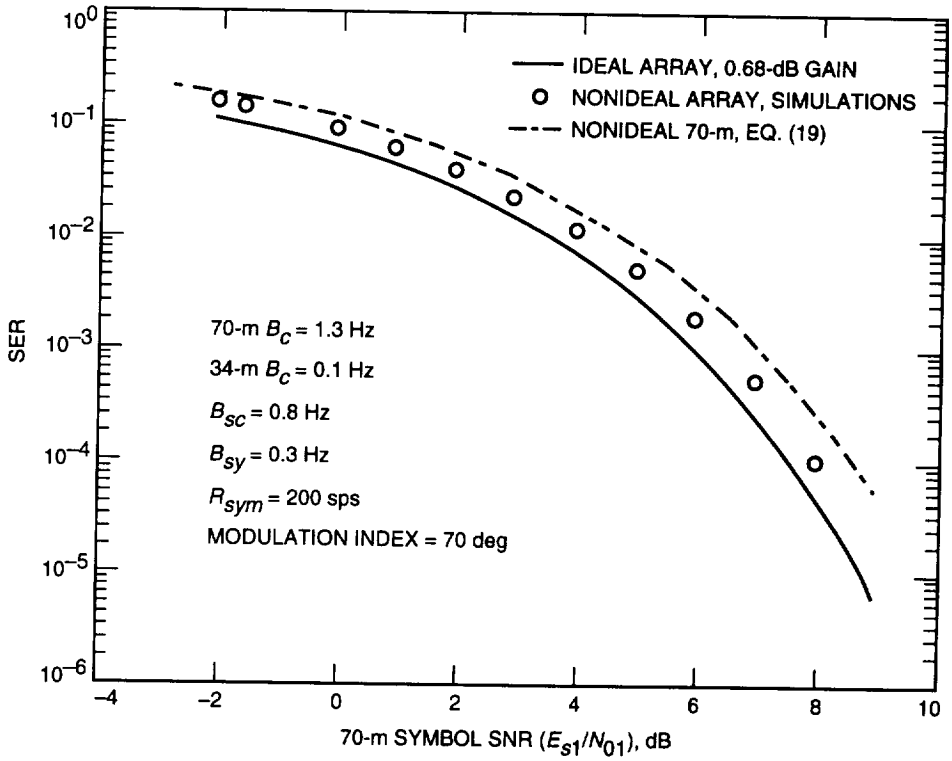


**Fig. 20. SER (simulations).**

## Acknowledgments

We would like to thank Dr. D. Divsalar for reviewing this article and Prof. H. Tan for many helpful discussions.

## References

[1] A. Mileant and S. Hinedi, "Overview of Arraying Techniques for Deep Space Communications," *IEEE Trans. on Comm.*, vol. 42, nos. 2/3/4, pp. 1856–1865, February/March/April 1994.

[2] D. Divsalar, "Symbol Stream Combining Versus Baseband Combining for Telemetry Arraying," *The Telecommunications and Data Acquisition Progress Report 42-74, April–June 1983*, Jet Propulsion Laboratory, Pasadena, California, pp. 13–28, August 15, 1983.

[3] S. Million, B. Shah, and S. Hinedi, "A Comparison of Full-Spectrum and Complex Symbol Combining Techniques for the Galileo S-Band Mission," *The Telecommunications and Data Acquisition Progress Report 42-116, October–December 1993*, Jet Propulsion Laboratory, Pasadena, California, pp. 128–162, February 15, 1994.

[4] W. Rafferty, S. Slobin, C. Stelzried, and M. Sue, "Ground Antennas in NASA's Deep Space Telecommunications," *Proceedings of the IEEE*, vol. 82, no. 5, pp. 636–645, May 1994.

[5] S. Aguirre, "Acquisition Times of Carrier Tracking Sampled Data Phase Locked Loops," *The Telecommunications and Data Acquisition Progress Report 42-84, October–December 1985*, Jet Propulsion Laboratory, Pasadena, California, pp. 88–93, February 15, 1986.

[6] J. Yuen, *Deep Space Telecommunications Systems Engineering*, New York: Plenum Press, 1983.

[7] W. J. Hurd and S. Aguirre, "A Method to Dramatically Improve Subcarrier Tracking," *IEEE Trans. on Commun.*, vol. 36, pp. 238–243, February 1988.

[8] M. K. Simon, "Analysis of the Steady-State Phase Noise Performance of a Digital Data-Transition Tracking Loop," *Space Program Summary 37-55*, vol. 3, Jet Propulsion Laboratory, Pasadena, California, pp. 54–62, February 1969.

[9] M. K. Simon, S. M. Hinedi, and W. C. Lindsey, *Digital Communication Techniques–Signal Design and Detection*, New Jersey: Prentice-Hall Inc., 1994.

[10] H. Wilck, "A Signal Combiner for Antenna Arraying," *JPL Deep Space Network Progress Report 42-25*, Jet Propulsion Laboratory, Pasadena, California, pp. 111–117, February 15, 1975.

[11] M. Shihabi and H. Tan, "Open Loop Residual Carrier Arraying with Baseband Combining," *IEEE GLOBECOM '94*, San Francisco, California, pp. 1040–1044, November 27–December 1, 1994.

[12] D. Divsalar and J. Yuen, "Carrier Arraying with Coupled Phase-Locked Loops for Tracking Improvement," *IEEE Trans. on Comm.*, vol. 30, no. 10, pp. 2319–2328, October 1982.

[13] T. Pham, M. Simon, T. Peng, M. H. Brockman, S. Kent, and R. Weller, "A Carrier-Arraying Demonstration at Goldstone for Receiving Pioneer 11 Signals," *The Telecommunications and Data Acquisition Progress Report 42-106, April–June 1991*, Jet Propulsion Laboratory, Pasadena, California, pp. 307–334, August 15, 1991.

[14] W. C. Lindsey and C. L. Weber, "On the Theory of Automatic Phase Control," *Stochastic Optimization and Control*, edited by H. F. Karreman, New York: John Wiley & Sons, Inc., 1968.

[15] C. L. Weber and J. J. Stein, "Cascaded Phase Locked Loops," *Proceedings of National Electronic Conference*, vol. 24, pp. 181–186, December 1968.

[16] J. Yuen, *Theory of Cascaded and Parallel Tracking Systems with Applications*, Ph.D. Dissertation, University of Southern California, Los Angeles, June 1971.

# Appendix

# Performance of Two Cascaded Phase-Locked Loops

The analysis of cascaded loops was considered in the past by several authors [14–16] for the purpose of determining accurate two-way Doppler and phase measurements between an antenna and a spacecraft in order to determine the relative position and velocity of the spacecraft. Here, in the carrier-aiding scheme, we are interested in determining accurately the loop SNR of the aided loop and the joint pdf of the two carrier phase error processes. Therefore, to accomplish that, we can apply the results of [14], keeping in mind that, in our case, the two cascaded loops are both in the downlink.

The proposed solution in [15], which is based on Fokker–Planck techniques and verified by simulation, takes on the following form:

$$p(x_1, x_2) = \frac{\exp\{a_2 \cos[(x_2 - m_2) - a(x_1 - m_1)] + a_1 \cos(x_1 - m_1)\}}{(2\pi)^2 I_0(a_2) I_0(a_1)} \tag{A-1}$$

where

$$\left.\begin{aligned} a_1 &= \frac{1}{\sigma_1^2} \\ a_2 &= [\sigma_2^2(1-\rho^2)]^{-1} \\ a &= \frac{\eta\sigma_2}{\sigma_1} \end{aligned}\right\} \tag{A-2}$$

within the region

$$-\pi \le x_i \le \pi \text{ for } i = 1, 2$$

and

$$(x_1, x_2) = \begin{cases} (\hat{\theta}_1, \hat{\theta}_2) & \text{then } (m_1, m_2) = (\theta_1, \theta_2 + \hat{\theta}_1) \\ (\hat{\phi}_1, \hat{\phi}_2) & \text{then } (m_1, m_2) = (0, 0) \end{cases}$$

The $\sigma_1^2$, $\sigma_2^2$, $\rho$, $m_1$, and $m_2$ are the parameters of the two-dimensional Gaussian density to which either $p(\hat{\theta}_1, \hat{\theta}_2)$ or $p(\hat{\phi}_1, \hat{\phi}_2)$ converge at high SNR, which must be determined in terms of the cascaded loop system parameters in order to characterize the joint density function as given in Eq. (A-1). The results that are stated here are specialized to second-order loops with imperfect integrators and damping parameters equal to 2.

# A High-Speed Photonic Clock and Carrier Regenerator

X. S. Yao and G. Lutes
Communications Systems Research Section

*As data communications rates climb toward 10 Gbits/s, clock recovery and synchronization become more difficult, if not impossible, using conventional electronic circuits. The high-speed photonic clock regenerator described in this article may be more suitable for such use. This photonic regenerator is based on a previously reported photonic oscillator capable of fast acquisition and synchronization. With both electrical and optical clock inputs and outputs, the device is easily interfaced with fiber-optic systems. The recovered electrical clock can be used locally and the optical clock can be used anywhere within a several kilometer radius of the clock/carrier regenerator.*

## I. Introduction

In high-speed fiber-optic communications systems, the ability to recover the clock from the incoming random data is essential. The recovered clock must be in precise synchronism with the incoming data and is used in further signal processing systems, such as regenerative repeaters, time division switching systems, and demultiplexers.

Conventional clock recovery devices are generally based on electronic phase-locked loops (PLLs) [1]. These devices may not be suited for the high-speed fiber-optic communications system because of their relatively slow speed, slow acquisition time, narrow tracking range, inability to be tuned over a wide range of frequencies, and non-optical inputs and outputs. Having optical inputs and outputs is important because it makes interfacing with a fiber-optic system easier.

All optical clock recovery schemes proposed by many authors [2–6] are based on injection locking a pulsed laser with the incoming data stream, wherein the pulsed laser has a nominal pulsation rate close to the incoming data rate. In one scheme, the pulsed laser [2–4] is a mode-locked fiber ring laser, and the input data modulates the laser cavity length or loss via the optical nonlinear effect. Because optical nonlinearity is used, the intensity of the injection data has to be high and is, therefore, not practical in many applications. In another scheme, the pulsed laser is a self-pulsating semiconductor laser [5,6] where the self-pulsation is caused by self-Q-switching within the device. The pulsation rate can be controlled by varying the current to the device. The problems associated with such a device are the relatively low speed (a few GHz) and relatively high noise.

Although the concept of all optical systems is attractive, the majority of present and future systems will be hybrid, meaning that the system can be controlled and accessed both optically and electronically.